

# Cosmography and constraints on the equation of state of the Universe in various parametrizations

Alejandro Aviles,<sup>1,2,\*</sup> Christine Gruber,<sup>3,†</sup> Orlando Luongo,<sup>1,4,5,‡</sup> and Hernando Quevedo<sup>1,4,§</sup>

<sup>1</sup>*Instituto de Ciencias Nucleares, Universidad Nacional Autónoma de México, AP 70543, México, DF 04510, Mexico*

<sup>2</sup>*Departamento de Física, Instituto Nacional de Investigaciones Nucleares, AP 70543, México, DF 04510, Mexico*

<sup>3</sup>*Institut fuer Theoretische Physik, Freie Universitaet Berlin, Arnimallee 14, D-14195 Berlin, Germany*

<sup>4</sup>*Dipartimento di Fisica and Icria, Università di Roma "La Sapienza", Piazzale Aldo Moro 5, I-00185, Roma, Italy*

<sup>5</sup>*Dipartimento di Scienze Fisiche, Università di Napoli "Federico II", Via Cinthia, I-80126, Napoli, Italy*

We use cosmography to present constraints on the kinematics of the Universe, without postulating any underlying theoretical model. To this end, we use a Monte Carlo Markov Chain analysis to perform comparisons to the supernova Ia Union 2 compilation, combined with the Hubble Space Telescope measurements of the Hubble constant, and the Hubble parameter datasets. We introduce a sixth order cosmographic parameter and show that it does not enlarge considerably the posterior distribution when comparing to the fifth order results. We also propose a way to construct viable parameter variables to be used as alternatives of the redshift  $z$ . These can overcome both the problems of divergence and lack of accuracy associated with the use of  $z$ . Moreover, we show that it is possible to improve the numerical fits by re-parameterizing the cosmological distances. In addition, we constrain the equation of state of the Universe as a whole by the use of cosmography. Thus, we derive expressions which can be directly used to fit the equation of state and the pressure derivatives up to fourth order. To this end, it is necessary to depart from a pure cosmographic analysis and to assume the Friedmann equations as valid. All our results are consistent with the  $\Lambda$ CDM model, although alternative fluid models, with nearly constant pressure and no cosmological constant, match the results accurately as well.

PACS numbers: 98.80.-k, 98.80.Jk, 98.80.Es

## I. INTRODUCTION

Ever since the pioneering works of two separate groups in 1998 [1], cosmological observations indicate a late time accelerated Universe. More recently, additional evidence coming from other experiments [2, 3] confirms that the Universe is going through an accelerated expansion. Thus, the existence of the acceleration is assumed to be a consolidated feature of cosmology [4]. Unfortunately, the physical mechanism from which this cosmic speed up originates is still unclear; the common way to deal with this is to assume, in addition to the standard matter term, the existence of a further exotic fluid which influences the dynamics of the Universe [5–8]. Due to the lack of knowledge on the physical nature of this fluid, we usually refer to it as dark energy (DE). So far, DE is only observationally witnessed, while the micro-physics behind it remains totally undisclosed [9–13]. One of the most dubious properties of DE is that it exhibits a negative equation of state (EoS) parameter, counteracting the attractive action of gravity [14]. The need of a negative pressure hints at the non-baryonic nature of DE, since no common matter is expected to show such a property. Besides that, the total amount of cosmological matter in the Universe appears to be dominated by a non-baryonic

(cold) dark matter (DM) component, which accounts for about 23% of the total energy content of the Universe. On the other hand, the common baryonic matter in the Universe only accounts for 4% of the whole energy content. This shows that the standard visible matter is actually not enough to guarantee the stability of structure observed at different astrophysical and cosmological scales, and DM cannot be ignored for the dynamics of the whole Universe [15, 16].

Consequently, our knowledge of the correct cosmological model seems to be lacking of some ingredients. However, in order to investigate the effects of DE and DM in Einstein's equations, one introduces a common energy momentum tensor with a pressureless term, i.e.  $P_m = 0$ , describing the total visible and non-visible matter content, and an additional term with a negative pressure to represent DE [17]. Together with these assumptions, one generally considers a homogeneous and isotropic Universe, depicted by the Friedmann-Robertson-Walker (FRW) metric,  $ds^2 = -c^2 dt^2 + a(t)^2 (dr^2/(1 - kr^2) + r^2 \sin^2 \theta d\phi^2 + r^2 d\theta^2)$ . In addition, observations of the large scale geometry of the Universe suggest a spatially quite flat Universe, so hereafter we will assume  $k = 0$ . To account for the effects of DE, the simplest and most tested assumption deals with the introduction of a cosmological constant term  $\Lambda$  into the Einstein equations. According to quantum field theory, the constant is interpreted as a vacuum energy contribution, and naturally leads to a negative EoS parameter with a positive energy density and negative pressure. The corresponding model, which is straightforwardly derived by solving

\*Electronic address: aviles@ciencias.unam.mx

†Electronic address: chrisgruber@physik.fu-berlin.de

‡Electronic address: orlando.luongo@roma1.infn.it

§Electronic address: quevedo@nucleares.unam.mx

the Einstein equations with the cosmological constant, is known as  $\Lambda$ CDM [18], a model which by now achieved the status of the standard cosmological model. The reason which induces cosmologists to assume this particular model to be the standard one is that it excellently fits all observational data with high precision [19, 20]. Moreover, it is only relying on a remarkably small number of cosmological parameters, without any *ad hoc* additional terms [21]. Unexpectedly, observations show that both the magnitudes of matter and  $\Lambda$  are comparable at our time. Indicating with  $\Omega_m$  and  $\Omega_\Lambda$  the magnitudes of matter and DE respectively, observational bounds show that  $\Omega_\Lambda/\Omega_m \approx 2.7$ . This feature implies a strange and unexpected coincidence problem –because DE is expected to evolve separately from matter, it is quite astonishing to imagine that near the present time the two magnitudes should be so close to each other.

On the other hand, another uncomfortable shortcoming plagues the standard model. The observational limits on the magnitude of the cosmological constant disagree with the predicted value for about  $10^{123}$  orders of magnitude, leading to a serious fine-tuning problem [22]. This deeply disturbs the otherwise appealing picture of a cosmological constant and, together with the coincidence problem, dramatically afflicts the standard cosmological paradigm. Despite its success in explaining the observational data, the  $\Lambda$ CDM model is therefore theoretically incomplete<sup>1</sup>, or at least not well understood. Motivated by these defects, a *mare magnum* of different models has been proposed during the last decades; as a short sample see [25] and references therein. In this work we wonder whether the cosmological constant must be considered as the real unique explanation of DE, or if there exists a hidden mechanism behind the nature of the cosmic speed up. An enticing way to understand if  $\Lambda$ CDM is the favorite candidate for DE is represented by the analyses through model independent tests. Such procedures should be able to disclose the fundamental nature of DE without postulating a certain model *a priori*. In this way, it would be possible to analyze the dynamics of the Universe without imposing a cosmological constant from the beginning. If  $\Lambda$  really exists, no significant deviations from a constant EoS must be found by model-independent tests. As a consequence, it is necessary to inquire how much of modern cosmology is really independent of the Friedmann equations [26, 28]. In other words, distinguishing between kinematics and dynamics is viewed as a tool to discriminate fairly among models, in order to reveal the correct cosmological paradigm.

Surely one of the most powerful model independent approaches is represented by cosmography [29]. Cosmography, sometimes also referred to as cosmo-kinetics, was

first discussed by Weinberg in [19] and then extended by Visser in [26]. The underlying philosophy of cosmography is to involve the cosmological principle only. So, the FRW metric is the only ingredient that cosmography uses for obtaining bounds on the observable Universe. Cosmography permits us to infer how much DE or alternative components are required in regard to satisfy the Einstein equations. The idea is to expand some observables such as the cosmological distances or the Hubble parameter, into power series, and relating cosmological parameters directly to these observable quantities. In doing so, it is possible to appraise which models behave fairly well and which ones should be discarded as a consequence of not satisfying the basic demands introduced by cosmography. So cosmography strives for the development of a procedure able to constrain the kinematics of the Universe.

In this paper, we present an extension of the promising approach debated in Visser et al. [29]; we devote our efforts both to constraining  $\Lambda$ CDM and investigating whether it is the only possibility to explain the cosmological acceleration, or whether there are prominent alternatives [30]. In particular, we adopt the idea of cosmography developed in [26, 29, 31–34] and we improve it, by assuming an extended class of fitting quantities, assembled by a number of different cosmological distances. For theoretical reasons, which we will discuss in the next sections, we introduce new parameterizations of the redshift variable besides  $z$ , in order to improve the fitting procedure. These parameterizations are designed to reduce the problems associated to the experimental analysis at redshift  $z > 1$ . Thence, we make use of the most recent data of the Union 2 supernovae Ia (SNeIa), of the Hubble Space Telescope (HST) measurements of the Hubble factor, and of the  $H(z)$  compilations [35], through a Markov Chain Monte Carlo (MCMC) method, by modifying the publicly available code CosmoMC [36]. Afterwards, we also include a parametrization of the cosmological distances in terms of the EoS of the Universe as a whole and of their pressure derivatives. This allows us to directly fit the EoS of the Universe without having to undergo disadvantageous error propagation. In doing this, we assume the validity of the cosmological principle, and of General Relativity, since for this analysis it is necessary to invoke the Friedmann equations. This gives us certain constraints on the EoS and on the pressure derivatives in the framework of General Relativity.

The paper is organized as follows. In Sec. II we discuss the physics behind the concept of cosmography and its implications for modern cosmology in more detail; we introduce the new cosmographic coefficient  $m$ , and discuss how to build up a viable alternative parametrization to the redshift  $z$ . We then propose three new parameterizations and we study their properties, in view of the fitting procedure. In Sec. III we apply these recipes and present the results of the cosmographic fits by a numerical MCMC analysis. Section IV deals with the concept of the EoS; in particular we relate the EoS and the derivatives of pressure to the luminosity distance, in order to

---

<sup>1</sup> Moreover, nearly all the extensions of it appear to fail as well. For a recent and mentionable alternative, which naturally extends  $\Lambda$ CDM in general relativity, conforming to all the experimental bounds, see [16, 23, 24].

carry out a direct fit to cosmological data. We use these results to derive constraints on  $\Lambda$ CDM and the most generic DE model, characterized by the function  $G(z)$ , reducing to  $G(z=0) = 1 - \Omega_m$  at  $z=0$ . In Sec. V finally we draw conclusions and give an outlook to further paths of investigations.

## II. THE ROLE OF COSMOGRAPHY

In this section we focus on the role of cosmography in modern cosmology. Its aim is the study of the kinematic quantities, characterizing the cosmological scenario. For this reason, cosmography is also called *cosmo-kinetics*, or kinematics of the Universe. We therefore limit ourselves to the smallest number of assumptions possible. First, we presume the validity of the cosmological principle. Second, we suppose that the EoS of the Universe is determined by a non-specified number of different cosmological fluids<sup>2</sup>. We assume that the total pressure of these fluids, namely  $P$ , can be written as  $P = \sum_i P_i$ , and its total EoS parameter  $\omega = \sum_i P_i / \sum_i \rho_i$ . Here the index  $i$  runs over all the involved cosmological fluids. Following these assumptions, the paradigm of cosmography was first developed by Weinberg [19], who proposed to expand the scale factor in terms of a Taylor series around the present time  $t_0$ <sup>3</sup>. Following these recipes, it is natural to expect that many other physical quantities of interest, apart from  $a(t)$ , can be expanded as well. The power series coefficients in the expansion of the scale factor are known in the literature as cosmographic series (CS), when evaluated at our time  $t_0$ ; these quantities are related to the scale factor derivatives.

A feasible consequence of this prescription is that cosmography does not depend on the choice of a cosmological model. As a matter of fact, almost all cosmological tests assume *a priori* that the model under consideration is statistically favored; however, this creates a degeneracy among models and often it remains difficult to understand which model is really favored. Cosmography is, among various cosmological tests, one of the ways to alleviate that degeneracy. However, although cosmography is reviewed as a model independent procedure, a few words should be spent regarding the role of the spatial curvature,  $k$ . In particular, modern cosmological data are not enough at present to fix stringent convergence limits on the CS and  $k$ . It is possible to show that the term proportional to the (present) “variation of acceleration”,

i.e.  $j_0$ , cannot be measured alone. Defining the curvature density as  $\Omega_k \equiv \Omega_0 - 1$ , where  $\Omega_0$  represents the total density of the Universe, then one measures  $j_0 + \Omega_0$  [37]. Motivated by WMAP 7 results [20], we propose here to restrict the analysis to the spatially flat case, in which  $k=0$ . This naturally overcomes the dependence of  $j_0$  on  $\Omega_0$ , letting cosmography be independent of any particular cosmological framework.

Now we have all the ingredients to expand the scale factor into a series, yielding

$$\begin{aligned} a(t) = & a_0 \cdot \left[ 1 + \frac{da}{dt} \Big|_{t_0} (t - t_0) \right. \\ & + \frac{1}{2!} \frac{d^2 a}{dt^2} \Big|_{t_0} (t - t_0)^2 + \frac{1}{3!} \frac{d^3 a}{dt^3} \Big|_{t_0} (t - t_0)^3 \\ & + \frac{1}{4!} \frac{d^4 a}{dt^4} \Big|_{t_0} (t - t_0)^4 + \frac{1}{5!} \frac{d^5 a}{dt^5} \Big|_{t_0} (t - t_0)^5 \\ & \left. + \frac{1}{6!} \frac{d^6 a}{dt^6} \Big|_{t_0} (t - t_0)^6 + \mathcal{O}((t - t_0)^7) \right], \quad (1) \end{aligned}$$

where we truncated the series at the sixth order in  $\Delta t \equiv t - t_0$ . Here, we assume that  $t - t_0 > 0$ . Moreover, the constant  $a_0$  is the scale factor evaluated today. Without loss of generality, it is licit to identify hereafter  $a_0 = 1$ . Equation (1) can be recast as

$$\begin{aligned} a(t) = & 1 - H_0 \Delta t - \frac{q_0}{2} H_0^2 \Delta t^2 - \frac{j_0}{6} H_0^3 \Delta t^3 + \frac{s_0}{24} H_0^4 \Delta t^4 \\ & - \frac{l_0}{120} H_0^5 \Delta t^5 + \frac{m_0}{720} H_0^6 \Delta t^6 + \mathcal{O}(\Delta t^7), \quad (2) \end{aligned}$$

with the definition of the cosmographic coefficients as

$$\begin{aligned} H &\equiv \frac{1}{a} \frac{da}{dt}, & q &\equiv -\frac{1}{aH^2} \frac{d^2 a}{dt^2}, \\ j &\equiv \frac{1}{aH^3} \frac{d^3 a}{dt^3}, & s &\equiv \frac{1}{aH^4} \frac{d^4 a}{dt^4}, \\ l &\equiv \frac{1}{aH^5} \frac{d^5 a}{dt^5}, & m &\equiv \frac{1}{aH^6} \frac{d^6 a}{dt^6}. \end{aligned} \quad (3)$$

Having an expansion for  $a(t)$  is equivalent to having an expansion of the redshift  $z$ , in terms of  $H_0 \Delta t$  (see [38]).

As previously stressed, Eqs. (3), if evaluated at our time, are referred to as the CS. The subscript “0” in Eq. (2) indicates that the coefficients are evaluated at  $t = t_0$ . In particular, each term has its own specific physical interpretation. For example,  $q$ , the so-called acceleration parameter, specifies whether the Universe is accelerating or decelerating, depending on the sign. An accelerating Universe leads to  $-1 \leq q_0 < 0$ . On the contrary, a positive  $j_0$  implies that  $q$  changes sign as the Universe expands, and so forth for all the rest of the parameters. We usually attribute the names of jerk and snap to  $j$  and  $s$  respectively; so far, no universal name is associated to  $l$ . Here, we additionally introduce  $m$  as a further higher

<sup>2</sup> These fluids include matter, radiation, curvature, dark energy and so forth.

<sup>3</sup> Instead of the scale factor, also the Hubble parameter or the luminosity distance could be expanded. At late times it is allowed to neglect radiation within the energy momentum tensor in Einstein’s equations. In addition, as will be clarified later, we superimpose a spatially flat geometry, in accordance with the most recent observations.

order term. It is useful to combine the CS among themselves and express them in terms of each other, yielding

$$\begin{aligned}
q &= -\frac{\dot{H}}{H^2} - 1, \\
j &= \frac{\ddot{H}}{H^3} - 3q - 2, \\
s &= \frac{H^{(3)}}{H^4} + 4j + 3q(q+4) + 6, \\
l &= \frac{H^{(4)}}{H^5} - 24 - 60q - 30q^2 - 10j(q+2) + 5s, \\
m &= \frac{H^{(5)}}{H^6} + 10j^2 + 120j(q+1) + \\
&\quad 3[2l + 5(24q + 18q^2 + 2q^3 - 2s - qs + 8)].
\end{aligned} \tag{4}$$

Here, the dots and the numbers in brackets indicate the derivatives with respect to the cosmic time. By converting the derivatives in Eq. (4) from time to redshift, and inverting the relations, we can obtain the Hubble parameter as an expansion in terms of redshift,  $H(z)$  (the results can be found in Appendix B). Analogously, we can also expand other observable physical quantities in order to fit the cosmological data with the obtained functions.

It would be interesting to expand commonly used notions of cosmological distances to the same order of the Taylor expansion as the scale factor before. To this end, let us now introduce several examples of distances between two objects in cosmology, following the prescriptions given in [31]. Here, we state the luminosity distance  $d_L$  and other four alternative distances, namely the photon flux distance  $d_F$ , the photon count distance  $d_P$ , the deceleration distance  $d_Q$  and the angular diameter distance  $d_A$ . These distances are defined as

$$\begin{aligned}
d_L &= a_0 r_0 (1+z) = r_0 \cdot \frac{1}{a(t)}, \\
d_F &= \frac{d_L}{(1+z)^{1/2}} = r_0 \cdot \frac{1}{\sqrt{a(t)}}, \\
d_P &= \frac{d_L}{(1+z)} = r_0, \\
d_Q &= \frac{d_L}{(1+z)^{3/2}} = r_0 \cdot \sqrt{a(t)}, \\
d_A &= \frac{d_L}{(1+z)^2} = r_0 \cdot a(t).
\end{aligned} \tag{5}$$

The last four notions of distances are less commonly used in literature. Besides the luminosity distance  $d_L$ , which gives the ratio of the apparent and the absolute luminosity of an astrophysical object, we consider the photon flux distance  $d_F$ , which is not calculated from the energy flux in the detector, but from the photon flux, which is experimentally easier to measure. The photon count distance  $d_P$  is based on the total number of photons arriving at the detector as opposed to the photon

rate. The so-called deceleration distance  $d_Q$  has been introduced in [26] without having an immediate physical meaning, but in return a very simple and practical dependence on the deceleration parameter  $q_0$ . Finally, the angular diameter distance  $d_A$  was defined in [19] as the ratio of the physical size of the object at the time of light emission and its angular diameter observed today. To completely determine the distance expansions, we still need to calculate  $r_0$ . It is defined as the distance  $r$  a photon travels from a light source at  $r = r_0$  to our position at  $r = 0$ . It is defined as<sup>4</sup>

$$r_0 = \int_t^{t_0} \frac{dt'}{a(t')}. \tag{6}$$

We can calculate this quantity by inserting the power series expansion for the inverse of the scale factor and integrating each term in the sum separately. Finally the results are used to complete the calculations of the cosmological distances in terms of the redshift  $z$ . We report in Appendix A 1 the expansions of all the distances in Eqs. (5) in terms of  $z$ . These results can be compared with those of [29], in which the authors truncated the series at a lower order. In particular, they claimed the need of using all the distances for a cosmographic test. In principle, this may be true, because all the various cosmological distances rely on the fundamental assumption that the total number of photons is conserved on cosmic scales. Hence, there is no reason to discard one distance for another one, since all of them fulfill this condition. Unfortunately, there exists a *duality problem* plaguing such distances [39]. This problem is so far an open question of observational cosmology [40]. On the other hand, it has been suggested that the luminosity distance  $d_L$  is fairly well adapted to the cosmological data used in combined tests with supernovae Ia and HST [41–43]. Even though this topic is still object of debate [44], unlike Cattoen and Visser [29] we limit our attention to  $d_L$  only. We motivate this choice with the above considerations on the good adaptation of  $d_L$  to the data, and with its general use in literature [45].

There are two main problems arising in the context of cosmography. In principle, the Taylor series is expected to diverge at  $z \geq 1$ . This is a consequence of the fact that we are expanding around  $z \sim 0$  and so when  $z > 1$ , we get problems with convergence. Moreover, the finite truncations we made represent only an approximation of the exact function, giving therefore possibly misleading results. Thus, while the second problem can be alleviated by expanding to higher orders in adding more coefficients, this measure can introduce divergences into the analysis. These issues are intimately connected to the problem of

---

<sup>4</sup> Here we have omitted a factor of  $c$  in the numerator; for now and for the rest of the theoretical calculations in this paper, we will assume  $c = 1$ .



systematic errors. In fact, if errors are large enough, it is possible that bad convergence may afflict the numerical results.

We improve the accuracy of our work by using the Union 2 compilation, which reduces the problem of systematics, easing the second problem. On the other hand, in order to overcome the first issue, different parameterizations of the fitting functions can be taken into account. The idea is to carry out the expansion with a different variable which is used *ad interim* and is constructed to be limited in a more stringent interval. While  $z \in [0, \infty]$ , a new variable should for example be restricted to the interval  $[0, 1]$ .

A fairly well-known possibility is represented by the variable

$$y_1 = \frac{z}{1+z}, \quad (7)$$

frequently used in literature [26, 27]. The limits in the past Universe, i.e.  $z \in [0, \infty]$ , read  $y_1 \in [0, 1]$ , while in the future, i.e.  $z \in [-1, 0]$ :  $y_1 \in [-\infty, 0]$ . Immediately we notice that  $y_1$  can be expanded as  $z$  before as  $y_1 = y_1(H_0\Delta t)$ ; then, it is feasible to invert it, having  $H_0\Delta t$  in terms of  $y_1$ . Then, we can express the distances as functions of  $y_1$  (for the results, see Appendix A 2).

Furthermore, we propose a way to construct other viable parameterizations of the redshift variable. To this end, we introduce below three new propositions, namely  $y_2$ ,  $y_3$  and  $y_4$ , as

$$\begin{aligned} y_2 &= \arctan\left(\frac{z}{z+1}\right) = \arctan(1-a), \\ y_3 &= \frac{z}{1+z^2}, \\ y_4 &= \arctan z, \end{aligned} \quad (8)$$

whose limits are, for  $z \in [0, \infty]$  :  $y_2 \in [0, \frac{\pi}{4}]$ ,  $y_3 \in [0, 0]$ ,  $y_4 \in [0, \frac{\pi}{2}]$  and  $z \in [-1, 0]$  :  $y_2 \in [\frac{\pi}{2}, 0]$ ,  $y_3 \in [-\frac{1}{2}, 0]$ ,  $y_4 \in [-\frac{\pi}{4}, 0]$  and in which we used the definition of the scale factor, i.e.  $a \equiv (1+z)^{-1}$ .

We adopted the arctan in the parameterizations of  $y_{2,4}$  because it behaves smoothly and it is suited to give well-defined limits at  $z \rightarrow \infty$ . On the contrary,  $y_3$  is a polynomial in  $z$ ; so apparently, we would not expect it to lead to significantly different fitting behavior, but just to represent an alternative worth investigating. Equations (8) can be expanded into Taylor series for  $z \ll 1$ , and then be inverted for  $y_{2,3,4}$  in order to give an expression for  $H_0\Delta t(y_{2,3,4})$ , up to sixth order. Then the distances as functions of  $y_{1,2,3,4}$  can be calculated as well (results see Appendices A 3-A 5).

By definition, all these parameterizations are built up to avoid divergences at  $z > 1$ . Thus, one can wonder whether all of them turn out to be equally suitable for constraining the CS. The answer can be partly predicted by comparing the supernova data of the luminosity distance, as in Fig. 1, for  $z$  and  $y_{1,2,3,4}$ . The worst example is clearly the redshift  $y_3$ . Its definition suggests that it

scales down more quickly, compared to the redshift  $z$ , as can also be seen in Fig. 1. This means that a region of  $z \in [0, 1.5]$  is reduced to a much smaller interval  $y_3 \in [0, 0.5]$ . Thereafter, we expect that, when the curve bends too quickly, the fits become more difficult. It follows that, as the curve trends become more extreme, a suppression of lower redshifts to the advantage of higher ones can occur. In other words,  $z \in [0, 0.5]$  weighs less than  $z \geq 0.5$ ; therefore, we guess that  $y_3$  would work better if all the cosmological data were for  $z \gg 1$ .

As it can be seen in Fig. 1, the luminosity distance curves of data points over redshift are slightly flexed, becoming steeper towards higher redshifts. Also the redshifts  $y_1$ ,  $y_2$  and  $y_4$  lead to steeper curves than  $z$ , however, redshift  $y_3$  behaves the most extreme. According to the cited criteria,  $y_3$  is the least suitable of redshift notions. This conjecture is also backed by the fitting results, which confirm that  $y_3$  does not work well in the application to SNeIa data. Another disadvantage of  $y_3$  is that it does not have a uniquely defined inverse. For these reasons, we decided to take it out of the analysis. Through similar arguments, we remove the second-worst redshift,  $y_2$ , as well. Summing up, in order to contrive a viable redshift parametrization, the following conditions must be satisfied:

1. The luminosity distance curve should not behave too steeply in the interval  $z < 1$ .
2. The luminosity distance curve should not exhibit sudden flexes.
3. The curve should be one-to-one invertible.

From Fig. 1, we notice that the last introduced redshift  $y_4$ , although still producing a steeper curve than  $z$ , is expected to work better than  $y_1$ . Thus, the rest of the analysis, including further calculations and fittings, is carried out for the redshifts  $z$ ,  $y_1$  and  $y_4$ .

### III. THE FITTING PROCEDURE AND THE COSMOGRAPHIC RESULTS

In Sec. II, we explained how to construct viable cosmological parameterizations to alleviate the problems associated to cosmography. To this end, we introduced  $y_4$  and we investigated its theoretical viability to fit the cosmological data. We now have all the ingredients to develop a MCMC procedure to find cosmographic constraints for the CS, using the three redshifts  $z$ ,  $y_1$  and  $y_4$  for the fitting analysis. We will include the sixth order of the CS, i.e.  $m_0$ , and particularly focus on the following aspects:

- We investigate whether redshift  $y_4$  is actually suitable to obtain accurate values of the CS, as theoretically predicted, and we explore the ranges of low and higher redshifts;

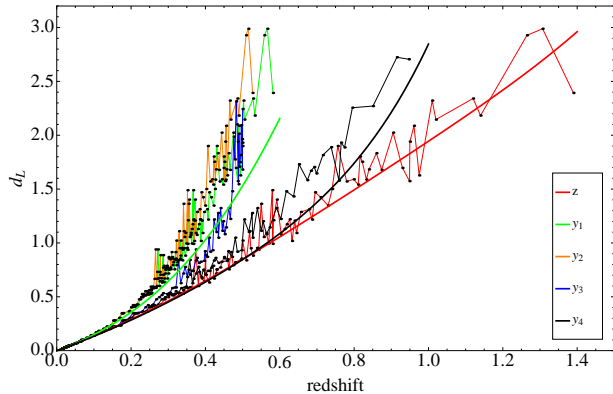


FIG. 1: (color online) Luminosity distance (in units of  $10^{26}$  m), over different redshifts  $z$  (red),  $y_1$  (green),  $y_2$  (orange),  $y_3$  (blue) and  $y_4$  (black).

- We analyze how well the introduced CS parameter  $m_0$  can be constrained, in particular, we examine whether its introduction significantly enlarges the dispersion of the estimation of the other parameters;
- We find out if the concordance model, i.e.  $\Lambda$ CDM, is in agreement with the cosmographically found numerical results.

For our purposes, we use the data of the SNeIa Union 2 compilation by the supernovae cosmology project [42]. We also adopt the HST measurements on 600 Cepheids, which impose a Gaussian prior on the Hubble parameter today of  $H_0 = 74.0 \pm 3.6$  km/s/Mpc [46], and the measurements of the Hubble parameter  $H(z)$  at twelve different redshifts ranging from  $z = 0.1$  to  $z = 1.75$  [47]. We divide our analysis into two sets of observations, namely set 1, which comprises Union 2 together with HST, and set 2, being the Union 2 dataset with both HST and  $H(z)$  measurements. For the sake of completeness, it is in order to cite recent works using gamma ray bursts (GRBs) as possible distance indicators [32, 33, 48]. However, considering GRBs in such analyses is mere speculation, since GRBs are not standard candles [49]. This approach seems to result in wrong estimations, or at least inadequate results. It will be shown that our results differ from those obtained by using GRBs; we will show a set of results in better agreement with  $\Lambda$ CDM than those obtained by using GRBs, which points to an inadequacy of the use of GRBs in cosmography. We also exclude observation data from baryonic acoustic oscillations from our analysis; we deem that introducing baryon acoustic oscillations means reducing the model-independence of the whole analysis [50].

In the following, we will use the CS combined together in three sets with different maximum order of parameters:

$$\begin{aligned} \mathcal{A} &= \{H_0, q_0, j_0, s_0\}, \\ \mathcal{B} &= \{H_0, q_0, j_0, s_0, l_0\}, \\ \mathcal{C} &= \{H_0, q_0, j_0, s_0, l_0, m_0\}. \end{aligned} \quad (9)$$

We expect a slower convergence of the last dataset, since the introduction of  $m_0$  can decrease the accuracy of convergence. To constrain the parameters, we use a Bayesian technique in which the best fits are those maximizing the likelihood function  $\mathcal{L} \propto \exp(-\chi^2/2)$ . Since the different observations are not correlated, the function  $\chi^2$  is simply given by the sum  $\chi^2 = \chi_{\text{Union 2}}^2 + \chi_{\text{HST}}^2 + \chi_{H(z)}^2$ . We explore the space of parameters with a MCMC approach, modifying the publicly available code CosmoMC [36]. We do the analysis for the three sets' parameter space, for the two sets of observations, and for each of the three considered redshifts. Accordingly, we perform 18 different constraint parameter analyses. To obtain the posterior samples we assume flat priors over the intervals  $-6 < q_0 < 6$ ,  $-20 < j_0 < 20$ ,  $-200 < s_0 < 200$ ,  $-500 < l_0 < 500$ , and  $-3000 < m_0 < 3000$ .

In Tables I, II, and III we show the best fits and their  $1\sigma$ -likelihoods for the redshifts  $z$ ,  $y_1$  and  $y_4$  respectively.

In Fig. 2 we compare the 1-dimensional marginalized posterior distributions for each parameter and each redshift for set 2 of observations. We note that the parameters  $l_0$  and  $m_0$  are not well constrained when using the redshift  $y_1$ . By introducing  $y_4$  it is possible to overcome this issue, obtaining good results on  $l_0$  and  $m_0$  as well. As expected, the redshift  $z$  appears to be statistically more favored than  $y_4$ . We confirm what we conjectured in Sec. II: the sixth order of the Hubble expansion in  $z$  works better than any other parametrization, if  $z \leq 1$ . Nonetheless,  $y_4$  should be taken seriously as a possible alternative to  $y_1$ , when  $z \geq 1$ . Similar conclusions have been drawn for the set 1; see Tables I, II, and III. The only caveat is that for set 1 the results appear to be less accurate as in the previous case.

We proceed to determine if the introduction of the parameters  $l_0$  and  $m_0$  is convenient. To this end, in Fig. 3 we plot the first four CS parameters' posterior distributions for the three parameter sets, comparing their statistical widths. We note that the dispersions are enlarged considerably when we add the  $l_0$  parameter; however, introducing  $m_0$  does not substantially broaden the posterior distributions; besides, the standard deviations of the posteriors are in a proportion  $1 : 2.28 : 1.92$  for  $j_0$  and  $1 : 5.66 : 8.38$  for  $s_0$ .

In Fig. 4 we present the summary of the results for the redshift  $y_4$  and parameter set  $\mathcal{C}$  by plotting the 2-dimensional contours and the likelihood samples.

TABLE I: Table of best fits and their likelihoods ( $1\sigma$ ) for redshift  $z$ , for the three sets of parameters  $\mathcal{A}$ ,  $\mathcal{B}$  and  $\mathcal{C}$ . Set 1 of observations is Union 2 + HST. Set 2 of observations is Union 2 + HST +  $H(z)$ .

Parameter	$\mathcal{A}$ , Set 1	$\mathcal{A}$ , Set 2	$\mathcal{B}$ , Set 1	$\mathcal{B}$ , Set 2	$\mathcal{C}$ , Set 1	$\mathcal{C}$ , Set 2
	$\chi^2_{min} = 530.1^b$	545.6	530.1	544.5	530.0	544.3
$H_0$	$74.35^{+7.39}_{-7.50}$	$74.22^{+5.23}_{-5.08}$	$73.77^{+8.36}_{-7.35}$	$74.20^{+5.01}_{-5.49}$	$73.72^{+8.47}_{-7.12}$	$73.65^{+5.92}_{-5.35}$
$q_0$	$-0.7085^{+0.6074}_{-0.5952}$	$-0.6149^{+0.2716}_{-0.2238}$	$-0.6250^{+0.5580}_{-0.4953}$	$-0.6361^{+0.3720}_{-0.3645}$	$-0.6208^{+0.4849}_{-0.6773}$	$-0.5856^{+0.3884}_{-0.3445}$
$j_0$	$1.605^{+6.738}_{-4.481}$	$1.030^{+0.722}_{-1.001}$	$0.392^{+4.585}_{-4.511}$	$0.994^{+1.904}_{-2.665}$	$-1.083^{+8.359}_{-2.218}$	$-0.117^{+3.621}_{-1.257}$
$s_0$	$2.53^{+60.61}_{-10.45}$	$0.16^{+1.45}_{-1.03}$	$-5.59^{+33.74}_{-34.55}$	$-1.47^{+4.20}_{-10.72}$	$-25.52^{+65.60}_{-10.90}$	$-7.71^{+14.77}_{-7.83}$
$l_0$	—	—	$-3.50^{+196.09}_{-89.19}$	$4.47^{+41.53}_{-8.47}$	<i>N.C.</i>	$8.55^{+23.39}_{-27.86}$
$m_0$	—	—	—	—	<i>N.C.</i>	$71.93^{+382.17}_{-315.76}$

Notes.

a.  $H_0$  is given in Km/s/Mpc.

b. *N.C.* means the results are not conclusive. The data do not constrain the parameters sufficiently.

TABLE II: Table of best fits and their likelihoods ( $1\sigma$ ) for redshift  $y_1$ , for the three sets of parameters  $\mathcal{A}$ ,  $\mathcal{B}$  and  $\mathcal{C}$ . Set 1 of observations is Union 2 + HST. Set 2 of observations is Union 2 + HST +  $H(z)$ .

Parameter	$\mathcal{A}$ , Set 1	$\mathcal{A}$ , Set 2	$\mathcal{B}$ , Set 1	$\mathcal{B}$ , Set 2	$\mathcal{C}$ , Set 1	$\mathcal{C}$ , Set 2
	$\chi^2_{min} = 530.1$	550.1	529.9	544.5	530.0	545.1
$H_0$	$74.05^{+7.90}_{-7.19}$	$75.25^{+4.72}_{-4.87}$	$73.68^{+7.77}_{-6.94}$	$73.30^{+5.59}_{-5.22}$	$73.91^{+7.60}_{-6.97}$	$74.49^{+5.07}_{-5.59}$
$q_0$	$-0.6633^{+0.5753}_{-0.6580}$	$-0.4106^{+0.2919}_{-0.5774}$	$-0.0004^{+0.2513}_{-1.6617}$	$-0.2652^{+0.5071}_{-0.7977}$	$-0.5360^{+0.8468}_{-0.8965}$	$-0.4624^{+0.5804}_{-0.8391}$
$j_0$	$1.268^{+6.986}_{-4.273}$	$-7.746^{+15.526}_{-2.252}$	$-13.695^{+30.901}_{-1.703}$	$-7.959^{+13.529}_{-5.228}$	$-1.646^{+11.637}_{-8.345}$	$-1.862^{+11.021}_{-5.397}$
$s_0$	$1.21^{+61.24}_{-9.24}$	$-88.91^{+57.62}_{-11.08}$	$-180.95^{+331.75}_{-18.93}$	$-112.63^{+156.60}_{-82.53}$	$-30.97^{+90.96}_{-43.47}$	$-16.95^{+73.68}_{-38.79}$
$l_0$	—	—	<i>N.C.</i>	<i>N.C.</i>	<i>N.C.</i>	<i>N.C.</i>
$m_0$	—	—	—	—	<i>N.C.</i>	<i>N.C.</i>

Notes.

a.  $H_0$  is given in Km/s/Mpc.

b. *N.C.* means the results are not conclusive. The data do not constrain the parameters sufficiently.

#### IV. THE CONNECTION BETWEEN THE CS AND THE EOS OF THE UNIVERSE

In Sec. I, we outlined that an expression for the EoS is naturally associated to each cosmological fluid in a given cosmological model; in particular, in thermodynamics the EoS characterizes the properties of such a fluid. Under the assumption of a specific gravitational model, the quest of understanding the expansion history of the Universe is equivalent to reproducing the correct EoS during different phases. Many physical mechanisms are hidden in the EoS parameter  $\omega$ . Finding the correct EoS has thus high importance in cosmology, because it offers a key to understanding the micro-physics associated to DE and/or DM. In this section we will assume that General Relativity gives a correct description of gravity at the scales under consideration.

Under the hypotheses of cosmography, we cannot *a priori* assume an EoS of the Universe, because we were not specifying any particular cosmological model at the beginning. We recall that the EoS of the Universe is given by  $\omega = \sum_i P_i / \sum_i \rho_i$ , where the subindex  $i$  refers to the different fluids that the Universe comprises. Hence,

to evaluate  $\omega$ , one needs to know the total pressure,  $P = \sum_i P_i$ , and the total density,  $\rho = \sum_i \rho_i$ . Even though we do not assume any EoS explicitly, it is possible to expand the pressure in terms of the cosmic time or redshift variables, i.e.  $z, y_1, y_4$ . By expanding the pressure into a series, it is possible to predict the values of its derivatives with respect to the cosmic time or the redshift variables. In fact, one can relate the derivatives of  $P$  to the CS; therefore, by substituting the values of CS in terms of these derivatives into the luminosity distances we are able to directly fit the parameters of the EoS of the Universe from luminosity distance data.

The reason of constraining the pressure derivatives lies in the possibility of discriminating among models; in principle, a model which does not satisfy such bounds can be easily discarded. The expansion of  $P$  in terms of the cosmic time is formally given by

$$P = \sum_{k=0}^{\infty} \frac{1}{k!} \frac{d^k P}{dt^k} \Big|_{t_0} (t - t_0)^k = \sum_{k=0}^{\infty} \frac{1}{k!} \frac{d^k P}{dy_i^k} \Big|_0 y_i^k, \quad (10)$$

where  $y_i = z, y_1, y_4$ . By truncating the series at the

TABLE III: Table of best fits and their likelihoods ( $1\sigma$ ) for redshift  $y_4$ , for the three sets of parameters  $\mathcal{A}$ ,  $\mathcal{B}$  and  $\mathcal{C}$ . Set 1 of observations is Union 2 + HST. Set 2 of observations is Union 2 + HST +  $H(z)$ .

Parameter	$\mathcal{A}$ , Set 1	$\mathcal{A}$ , Set 2	$\mathcal{B}$ , Set 1	$\mathcal{B}$ , Set 2	$\mathcal{C}$ , Set 1	$\mathcal{C}$ , Set 2
	$\chi^2_{min} = 530.3$	544.8	529.7	544.6	529.9	544.5
$H_0$	$74.55^{+7.54}_{-7.53}$	$73.71^{+5.29}_{-5.24}$	$73.95^{+7.99}_{-7.22}$	$73.43^{+6.05}_{-5.74}$	$74.12^{+8.27}_{-7.78}$	$73.27^{+6.86}_{-5.91}$
$q_0$	$-0.7492^{+0.5899}_{-0.6228}$	$-0.6504^{+0.4275}_{-0.3303}$	$-0.4611^{+0.5422}_{-0.6710}$	$-0.7230^{+0.5851}_{-0.4585}$	$-0.4842^{+2.7126}_{-0.9280}$	$-0.7284^{+0.6062}_{-0.4838}$
$j_0$	$2.558^{+7.441}_{-8.913}$	$1.342^{+1.391}_{-1.780}$	$-3.381^{+10.613}_{-2.149}$	$2.017^{+3.149}_{-3.022}$	$-1.940^{+8.041}_{-2.148}$	$2.148^{+3.414}_{-4.036}$
$s_0$	$9.85^{+74.69}_{-26.69}$	$3.151^{+3.920}_{-1.771}$	$-37.67^{+89.51}_{-60.10}$	$5.278^{+13.076}_{-14.732}$	$-13.48^{+71.65}_{-31.28}$	$2.179^{+42.126}_{-35.919}$
$l_0$	—	—	<i>N.C.</i>	$-0.13^{+96.75}_{-65.87}$	<i>N.C.</i>	$-11.60^{+193.88}_{-187.96}$
$m_0$	—	—	—	—	<i>N.C.</i>	$70.9^{+2497.8}_{-2254.5}$

Notes.

a.  $H_0$  is given in Km/s/Mpc.

b. *N.C.* means the results are not conclusive. The data do not constrain the parameters sufficiently.

fourth order, and the continuity equation

$$\frac{d\rho}{dt} + 3H(P + \rho) = 0, \quad (11)$$

and the Friedmann equation  $H^2 = \frac{1}{3}\rho$ , we can write down an explicit dependence of the pressure and the coefficients  $\frac{d^k P}{dt^k}$  on the CS as follows<sup>5</sup>

$$P = \frac{1}{3}H^2(2q - 1), \quad (12a)$$

$$\frac{dP}{dt} = \frac{2}{3}H^3(1 - j), \quad (12b)$$

$$\frac{d^2 P}{dt^2} = \frac{2}{3}H^4(j - 3q - s - 3), \quad (12c)$$

$$\frac{d^3 P}{dt^3} = \frac{2}{3}H^5 \left[ (2s + j - l + q(21 - j) + 6q^2 + 12) \right], \quad (12d)$$

$$\frac{d^4 P}{dt^4} = \frac{2}{3}H^6 \left[ j^2 + 3l - m - 144q - 81q^2 \right] \quad (12e)$$

$$- 6q^3 - 12j(2 + q) - 3s - 3qs - 60 \Big], \quad (12f)$$

where we evaluated the derivatives up to the order of  $m_0$ . We list the coefficients  $\frac{d^k P}{dz^k}$ ,  $\frac{d^k P}{dy_1^k}$  and  $\frac{d^k P}{dy_4^k}$  in Appendix C. For completeness, we write down the transformation laws between  $z, y_1, y_4$  and the cosmic time  $t$ , i.e.

$$\begin{aligned} \frac{\partial}{\partial t} &\rightarrow -(1+z)H \cdot \frac{\partial}{\partial z} \\ &\rightarrow -(1+y_1)H \frac{\partial}{\partial y_1} \\ &\rightarrow -\cos y_4(\cos y_4 + \sin y_4)H \frac{\partial}{\partial y_4}. \end{aligned} \quad (13)$$

In addition, by using Eq. (11), Eqs. (12) and the Friedmann equation  $H^2 = \frac{1}{3}\rho$ , we find the expression for the EoS parameter of the Universe as

$$\omega = \frac{2q - 1}{3}. \quad (14)$$

### A. Fitting the EoS

In this subsection, our goal is to obtain constraints on the EoS and the pressure derivatives by inverting Eqs. (12b) - (12f) and by rewriting the luminosity distance as a function of  $\omega_0, \frac{dP}{dy_i}\Big|_0, \frac{d^2 P}{dy_i^2}\Big|_0, \frac{d^3 P}{dy_i^3}\Big|_0, \frac{d^4 P}{dy_i^4}\Big|_0$ .

In other words, we use Eqs. (12b) - (12f) and (14), indicated henceforth by

$$\mathcal{D} = \left\{ \omega, P_1 := \frac{dP}{dy_i}, P_2 := \frac{d^2 P}{dy_i^2}, P_3 := \frac{d^3 P}{dy_i^3}, P_4 := \frac{d^4 P}{dy_i^4} \right\},$$

to express the vector  $\mathcal{CS} \equiv \{q_0, j_0, s_0, l_0, m_0\}$  as a function of the EoS parameter and the pressure derivatives,  $\mathcal{CS} = \mathcal{CS}(\omega_0, P_1, P_2, P_3, P_4)$ . The purpose is to plug those results into the expressions for the luminosity distance in order to find numerical best fit values of the new set of parameters, using  $d_L = d_L(\omega_0, P_1, P_2, P_3, P_4)$  in the numerical analysis.

In principle, there exists also an alternative procedure, which consists in taking the results already obtained for the CS and to propagate the errors through Eqs. (12b)-(12f), without performing another fitting procedure. But in choosing this way, we would face an unacceptable increase in the errors, as opposed to the direct fit of  $\{\omega_0, P_1, P_2, P_3, P_4\}$ . Thus, in order to reduce the error propagation, the simplest and most straightforward way is to evaluate the coefficients by a direct fit of the luminosity distance. The search for the best-fit values for the new set of parameters is performed by using the procedure of MCMC simulations developed in Sec. III.

For statistical reasons, we choose set 2 of observations, which is more complete and suitable for this kind of fit.

<sup>5</sup> Here in Eqs. (12) we are considering  $\frac{8\pi G}{3} = c = 1$  for brevity. These factors are considered again in the numerical simulations.



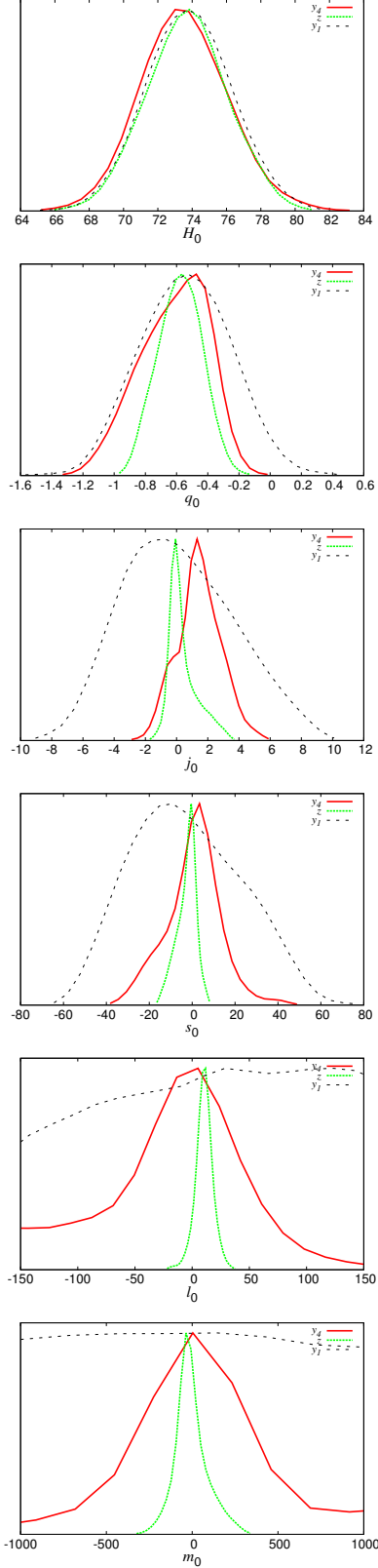


FIG. 2: (color online) 1-dimensional marginalized posteriors for the complete CS (parameter set  $\mathcal{C}$ ), using set 2 of observations (Union 2 + HST +  $H(z)$ ). Dotted (green) line is redshift  $z$ , dashed (black) line is  $y_1$  and solid (red) line is  $y_4$ .

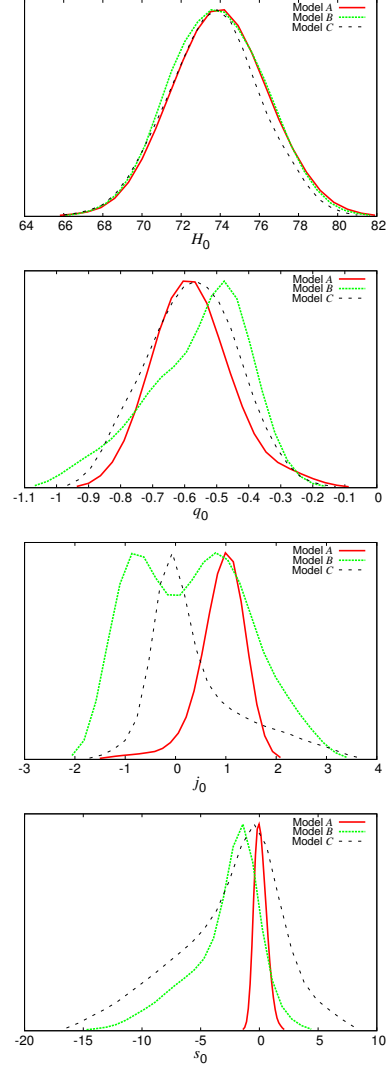


FIG. 3: (color online) 1-dimensional marginalized posteriors for  $H_0$ ,  $q_0$ ,  $j_0$  and  $s_0$ , using set 2 of observations (Union 2 + HST +  $H(z)$ ). Solid (red) line is parameter set  $\mathcal{A}$ , dotted (green) line is parameter set  $\mathcal{B}$  and dashed (black) line is parameter set  $\mathcal{C}$ .

The explicit expressions for the luminosity distance in terms of the different redshift parameters are reported for completeness in Appendix D. As in Sec. III we limit our analysis to  $d_L$ .

Figure 5 shows the obtained marginalized posteriors and in Tab. IV we present the summary of the results. We observe the same hierarchy of redshifts as in analysis of Sec. III; meaning that our new “redshift” introduction,  $y_4$ , appears to be statistically favored with respect to  $y_1$ .

TABLE IV: Table of mean values of the posteriors and their likelihoods ( $1\sigma$ ) for the three redshifts, using set 2 of observations (Union 2 + HST +  $H(z)$ ).  $P_1(z)$ ,  $P_1(y_1)$ ,  $P_1(y_4)$ ,  $P_2(z)$ ,  $P_2(y_4)$  and  $P_3(z)$  are in units of  $10^4 c^2/\kappa$ ,  $P_2(y_1)$  and  $P_4(y_4)$  in units of  $10^5 c^2/\kappa$ ,  $P_3(y_4)$  and  $P_4(z)$  in units of  $10^6 c^2/\kappa$ ,  $P_3(y_1)$  in units of  $10^7 \frac{c^2}{\kappa}$ , and  $P_4(y_1)$  in units of  $10^8 c^2/\kappa$ .

Parameter	Redshift $z$	Redshift $y_1$	Redshift $y_4$
$H_0$	$74.23^{+2.31}_{-2.36}$	$74.20^{+2.37}_{-2.36}$	$75.70^{+2.68}_{-2.66}$
$\omega_0$	$-0.7174^{+0.0922}_{-0.0964}$	$-0.7439^{+0.3085}_{-0.3222}$	$-0.7315^{+0.1193}_{-0.1373}$
$P_1$	$-0.209^{+0.347}_{-0.261}$	$-0.991^{+2.393}_{-2.213}$	$-0.228^{+0.506}_{-0.528}$
$P_2$	$0.988^{+2.012}_{-1.539}$	$-0.134^{+1.623}_{-1.729}$	$-0.246^{+4.133}_{-3.927}$
$P_3$	$0.630^{+4.010}_{-4.932}$	$0.205^{+0.294}_{-0.257}$	$0.217^{+0.625}_{-0.400}$
$P_4$	$-0.107^{+0.099}_{-0.170}$	$-0.150^{+0.209}_{-0.187}$	$-0.289^{+4.690}_{-6.112}$

Notes.  
a.  $H_0$  is given in Km/s/Mpc.

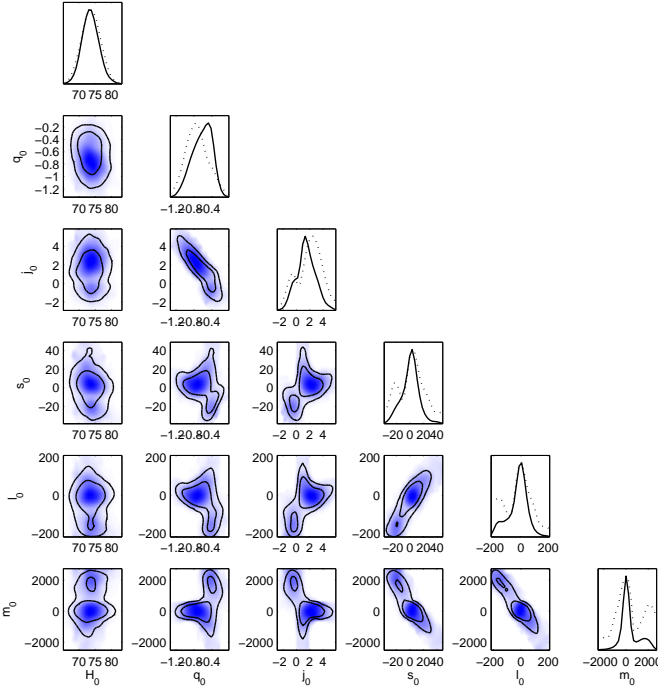


FIG. 4: Marginalized posterior constraints for redshift  $y_4$  and parameter set  $\mathcal{C}$ , using set 2 of observations (Union 2 + HST +  $H(z)$ ). The shaded region and the dotted lines show the likelihoods of the samples.

## B. Comparison with models

The results found by fitting the EoS show no conclusive evidence for a pressure varying in time, as shown by the  $1\sigma$  confidence levels in Tab. IV. This means that a negative constant pressure model is favored for depicting the cosmic speed up. Thus, the only two models accounting our results appear to be the concordance model and the vanishing speed of sound model (VSSM), proposed in [24, 30]. Their EoS parameters (neglecting radiation

components at late times) are  $\omega = -1/(1 + \Omega_m/\Omega_\Lambda a^{-3})$  and  $\omega = -1/(1 - (\xi - \Omega_m/\Omega_X)a^{-3})$ , for  $\Lambda$ CDM and VSSM respectively. They imply  $w_0 \simeq -0.73$  nowadays, by using the values of  $\Omega_m \simeq 0.27$  and  $\Omega_X \simeq 0.78$ ,  $\xi \simeq -0.025$ . These results have been confirmed by the present analysis.

Using set 2 of observations we worked out the  $\Lambda$ CDM model, which is for our purposes and the redshifts involved sufficiently described by the two parameters  $\{\Omega_m h^2, \theta\}$ . The philosophy is to estimate  $\Omega_m h^2$  and  $\theta$  by the Monte Carlo simulation and then substitute it into the CS in the  $\Lambda$ CDM model. To evaluate the CS for  $\Lambda$ CDM we use Eqs. (4) with  $H = H_0 \sqrt{\Omega_m(1+z)^3 + 1 - \Omega_m}$ , yielding

$$\begin{aligned}
 q_0 &= -1 + \frac{3}{2}\Omega_m, \\
 j_0 &= 1, \\
 s_0 &= 1 - \frac{9}{2}\Omega_m, \\
 l_0 &= 1 + 3\Omega_m - \frac{27}{2}\Omega_m^2, \\
 m_0 &= 1 - \frac{27}{2}\Omega_m^2 - 81\Omega_m^2 - \frac{81}{2}\Omega_m^3.
 \end{aligned} \tag{15}$$

Any significative tension between the CS values obtained in this way and the values derived before using cosmography would be an indication of the validity of a different theory, other than the concordance model. Table V gives the summary of the likelihoods of the estimated and derived parameters. Comparing these values with the ones obtained for models  $\mathcal{A}$ ,  $\mathcal{B}$  and  $\mathcal{C}$  we note that all our results are compatible with the  $\Lambda$ CDM model within the limits of error.

Now, we want to factorize the effects of DE by assuming a cold dark matter model, for which the Friedmann equation is given by

$$H = H_0 \sqrt{\Omega_m(1+z)^3 + G(z)},$$

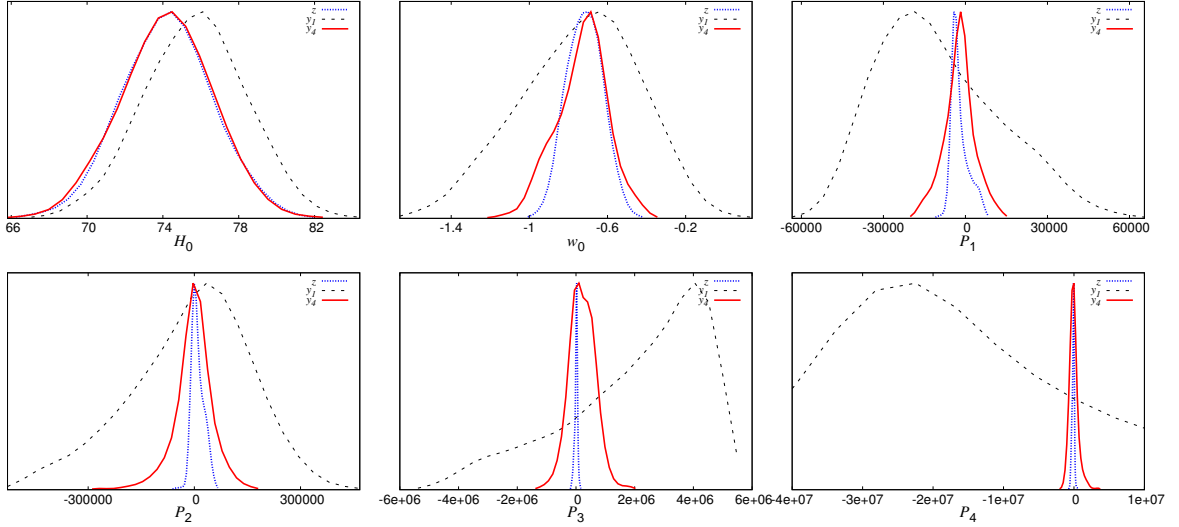


FIG. 5: (color online) 1-dimensional marginalized posteriors for the complete set of parameters of the EoS analysis, using set 2 of observations (Union 2 + HST +  $H(z)$ ). Dotted (blue) lines are used for  $z$ , dashed (black) lines for  $y_1$ , and solid (red) lines are for redshift  $y_4$ .

where  $G(z)$  models the corresponding DE term. We want to obtain constraints on  $G(z)$  and its derivatives with respect to redshifts for the present time  $z = 0$ . To this purpose we calculate the derivatives of the Hubble parameter as stated above with respect to the redshift and equate the results to the derivatives of the Hubble parameter in terms of the CS. Thus we obtained the derivatives of  $G(z)$  with respect to  $z$  (results see Appendix E). The same has been done for the redshifts  $y_1$  and  $y_4$ .

We can now use the numerically obtained values for the CS and the value  $\Omega_m = 0.274^{+0.015}_{-0.015}$  obtained by the WMAP7 collaboration [20] to calculate the  $G^{(k)}(y_i)$  and, by error propagation, their  $1\sigma$  error bars. The results can be found in Table VI. With these values it is possible to investigate the compatibility of a model of dark energy characterized by the function  $G(z)$  with the observational data at present time. The value of  $G(z)$  evaluated today can be estimated by the flat space condition, which implies  $G_0 = G(z = 0) = 1 - \Omega_m$  or, assuming Gaussian distributions,  $G_0 = 0.726^{+0.015}_{-0.015}$ .

From Table VI, we conclude that our results are consistent with a constant function  $G(z) = \Omega_\Lambda$ , which is the case of the  $\Lambda$ CDM model, or the case of an emergent constant as shown in [24, 30].

## V. CONCLUSIONS

In this work we emphasized the importance of constraining the Universe dynamics through the use of a model-independent procedure, which does not *a priori* assume the validity of a particular cosmological model. In other words, we used the so called cosmography, sometimes also referred to as cosmokinetics, to investigate the

TABLE V: Table of best fits and their likelihoods ( $1\sigma$ ) for the estimated (top panel) and derived (lower panel) parameters for the  $\Lambda$ CDM model, using set 2 of observations (union 2 + HST +  $H(z)$ ).

Parameter	Best Fit ( $1\sigma$ )
$\Omega_m h^2$	$0.1447^{+0.0181}_{-0.0174}$
$\theta$	$1.060^{+0.020}_{-0.022}$
$H_0$	$74.05^{+7.90}_{-7.19}$
$q_0$	$-0.6633^{+0.5753}_{-0.6580}$
$j_0$	1
$s_0$	$-0.2061^{+0.1772}_{-0.2015}$
$l_0$	$2.774^{+0.485}_{-0.382}$
$m_0$	$-8.827^{+2.263}_{-2.941}$

Notes.  
 $H_0$  is given in Km/s/Mpc. Here  $h$  is defined through the relation  $H_0 = 100 h$  km/s/Mpc, and  $\theta$  is the ratio of the sound horizon to the angular diameter distance at recombination.

kinematics of the Universe. By following [29], we performed an analysis combining theoretical derivations of cosmological distances and numerical data fitting, using the Union 2 compilation, together with the HST and the  $H(z)$  samples. For the fitting, we introduced new parameterizations in addition to the conventional redshift  $z$  to express the cosmological distances, underlining their importance to avoid divergences at high redshifts and to increase the accuracy of the analysis. Moreover, we proposed prescriptions to build up new viable parametrizations, able to overcome these issues.

We considered three further parameterizations, predicting that only one is really a viable option for fitting.

TABLE VI: Table of derived values and their likelihoods ( $1\sigma$ ) for the derivatives of  $G(y_i)$  for the three redshifts  $z, y_1, y_4$ , evaluated at  $t = t_0$ , using set  $\mathcal{C}$  of parameters and set 2 of observations (union 2 + HST +  $H(z)$ ).

Parameter	Best Fit for $z$ ( $1\sigma$ )	Best Fit for $y_1$ ( $1\sigma$ )	Best Fit for $y_4$ ( $1\sigma$ )
$G_0^{(1)}$	$0.0068^{+1.299}_{-1.23}$	$0.25^{+1.57}_{-1.87}$	$-0.2788^{+1.59994}_{-1.43882}$
$G_0^{(2)}$	$-2.22^{+4.61}_{-3.33}$	$-4.71^{+9.13}_{-8.8}$	$1.7384^{+4.88827}_{-4.94215}$
$G_0^{(3)}$	$13.65^{+8.04}_{-5.8}$	$0.7476^{+55.73}_{-49.34}$	$-3.43039^{+13.3403}_{-12.4275}$
$G_0^{(4)}$	$-17.24^{+35.27}_{-31.89}$	<i>N.C.</i>	$-16.2906^{+50.8794}_{-47.602}$
$G_0^{(5)}$	$-129.74^{+174.29}_{-130.39}$	<i>N.C.</i>	$-8.74593^{+332.408}_{-323.676}$

Notes.

a. *N.C.* means the results are not conclusive. The data do not constrain the parameters sufficiently.

By using the luminosity distance, i.e.  $d_L$ , in terms of the standard redshift  $z$ , of the alternative parametrization  $y_1 \equiv \frac{z}{1+z}$  and of the newly introduced  $y_4 = \arctan(z)$ , we obtained bounds on the cosmographic series. We moreover showed that there was no physical reason to use other notions of cosmological distances than the luminosity distance for evaluating bounds to the CS, as instead previously reported in [29]. The reason for this lies in the fact that  $d_L$  is adapted the best to the cosmological data under consideration. Then, we also showed that the most successful parametrization, apart from  $z$ , is represented by  $y_4$ , as theoretically predicted in Sec. II.

We carried out our fits up to the sixth order in the CS, introducing a further cosmographic parameter, namely  $m_0$ . In addition, we showed that fitting  $m_0$  together with  $q_0, j_0, s_0$  and  $l_0$ , is quite feasible to improve the accuracy of the analysis by fixing more stringent limits on the CS, as opposed to the expectation that an additional fitting parameter would significantly broaden the posterior distributions.

The analysis was done for three different sets of parameters (including parameters of the CS with different maximum order) and two different sets of observational data. We essentially found that our numerical results appear to be fairly well in agreement with a constant pressure associated to the fluid driving the cosmic acceleration. At first sight, this fluid could be obviously thought to originate from a cosmological constant, as depicted in the standard concordance model. Meanwhile, our constraints would be able, in future developments, to discard different classes of models, which do not satisfy the numerical bounds.

In addition to the numerical fits for the CS, we proposed a way to constrain both the EoS of the Universe as a whole and the derivatives of pressure, by fitting them directly from the luminosity distance, up to the order of the  $m_0$  coefficient. In other words, we rewrote  $d_L$  in terms of the EoS parameter and the pressure derivatives

and performed another MCMC analysis. To achieve this, it is necessary to depart from model independent cosmography by assuming a specific gravitational theory. We choose General Relativity as valid, and make use of the Friedmann equations. The corresponding results lead to a set of pressure derivatives compatible with zero within the  $1\sigma$  error propagation. Moreover, the EoS parameter  $\omega$  is compatible with the one predicted by  $\Lambda$ CDM, i.e.  $\omega = -1/(1 + \Omega_m/\Omega_\Lambda a^{-3})$ , obtaining  $\omega_0 \simeq -0.73$ . Even through the pressure derivative results seemed to confirm  $\Lambda$ CDM, they also left open the possibility that the viable model does not necessarily feature a cosmological constant, but dark energy with constant pressure and a varying barotropic factor, i.e. the VSSM model (as proposed in [24, 30]). In this model, which does not involve a cosmological constant, the predicted bounds are in agreement with our fitting results. Unfortunately, the strong degeneracy with  $\Lambda$ CDM in fitting data leaves open the question of which model is theoretically the favored one.

Future perspectives in this direction include using more accurate datasets and constraining the analysis at higher redshifts, in order to obtain limits able to discriminate among the two paradigms. We expect that this could give further insight into the issue of inferring the correct cosmological paradigm, employing a model-independent procedure, which does not need to specify a model a priori.

## Acknowledgments

A.A. acknowledges CONACYT for grant no. 215819. C.G. is supported by the Erasmus Mundus Joint Doctorate Program by Grant Number 2010-1816 from the EACEA of the European Commission. O.L. wants to thank Prof. A. Melchiorri for useful discussions.

[1] A. G. Riess *et al.*, *Astrophys. J.* **116**, 1009-1038 (1998); S. Perlmutter *et al.*, *Astrophys. J.* **517**, 565 (1999).

[2] Garnavich, P. M. *et al.*, *ApJ*, 509, 74 (1998); R. Rebolo *et al.*, *MNRAS* **353**, 747 (2004); A. C. Pope *et al.*, *As-*



- trophy. J. **607**, 655 (2004).
- [3] M. Tegmark *et al.* (SDSS Collaboration), Phys. Rev. D **74**, 123507 (2006); W. J. Percival, S. Cole, D. J. Eisenstein, R. C. Nichol, J. A. Peacock, A. C. Pope, and A. S. Szalay, MNRAS **381**, 1053 (2007).
- [4] S. M. Carroll, AIP Conf. Proc. **743**, 16 (2005); R. Amanullah *et al.*, Astrophys. J. **716**, 712 (2010).
- [5] V. Sahni and A. Starobinsky, Int. J. Mod. Phys. D **15**, 2105 (2006).
- [6] C. Clarkson, G. Ellis, J. Larena, and O. Umeh, Rep. Prog. Phys. **74**, 112901 (2011).
- [7] E. W. Kolb, S. Matarrese, A. Notari, and A. Riotto, Phys. Rev. D **71**, 023524 (2005).
- [8] S. Rasanen, JCAP **0611**, 003 (2006).
- [9] C. Bonvin, R. Durrer, and M. Kunz, Phys. Rev. Lett., **96**, 191302 (2006).
- [10] A. J. Albrecht *et al.*, arXiv:astro-ph/0609591 (2006).
- [11] A. Torres-Rodriguez and C. M. Cress, MNRAS **376**, 1831 (2007).
- [12] P. S. Corasaniti, T. Giannantonio, and A. Melchiorri, Phys. Rev. D **71**, 123521 (2005).
- [13] I. Maor and O. Lahav, JCAP **0507**, 003 (2005).
- [14] M. Li, X.-D. Li, S. Wang, and Y. Wang, Commun. Theor. Phys. **56** 525 (2011).
- [15] J. Einasto, AIP Conf. Proc. **1205**, 72-81 (2010); J. Einasto, arXiv:0901.0632 (2009); J. L. Feng, Ann. Rev. Astron. Astrophys. **48**, 495 (2010); I.A. Yegorova, A. Babic, P. Salucci, K. Spekkens, and A. Pizzella, arXiv:1110.1925 (2011).
- [16] A. Aviles and J. L. Cervantes-Cota, Phys. Rev. D. **84**, 083515 (2011).
- [17] M. Berry, *Principles of Cosmology and Gravitation*, Cambridge University Press, New York (1976).
- [18] T. Padmanabhan, Phys. Rep. **188**, 285 (1990).
- [19] S. Weinberg, *Cosmology*, Oxford Univ. Press, Oxford (2008).
- [20] E. Komatsu *et al.*, Astrophys. J. Supp. **192**, 18 (2011).
- [21] S. Tsujikawa, arXiv:1004.1493 (2010).
- [22] S. Weinberg, Rev. Mod. Phys. **61**, 1 (1989).
- [23] A. Balbi, M. Bruni, and C. Quercellini, Phys. Rev. D **76**, 103519 (2007).
- [24] O. Luongo, H. Quevedo, arXiv:1104.4758 (2011).
- [25] B. Ratra and P.J.E. Peebles, Phys. Rev. D **37**, 3406 (1988) R. Caldwell, R. Dave, and P. J. Steinhardt, Phys. Rev. Lett. **80**, 1582 (1998); G. R. Dvali, G. Gabadadze, and M. Porrati, Phys. Lett. B **485**, 208 (2000); C. Armendariz-Picon, V.F. Mukhanov, and P.J. Steinhardt, Phys. Rev. Lett. **85**, 4438 (2000); R. Micha and I. Tkachev, Phys. Rev. D **70**, 043538 (2004); E. J. Copeland, M. Sami, and S. Tsujikawa, Int. J. Mod. Phys. D **15**, 1753 (2006); T. Sotiriou and V. Faraoni, Rev. Mod. Phys. **82**, 451-497, (2010).
- [26] M. Visser, Gen. Rel. Grav. **37**, 1541 (2005).
- [27] S. Capozziello, R. Lazkoz, and V. Salzano, Phys.Rev. D **84**, 124061 (2011).
- [28] R. R. Caldwell and M. Kamionkowski, JCAP **0409**, 009 (2004); M. Visser, Class. Quant. Grav. **21**, 2603 (2004).
- [29] C. Cattoen and M. Visser, Phys.Rev. D **78**, 063501 (2008).
- [30] O. Luongo and H. Quevedo, Astroph. and Sp. Sci. **338**, 2, 345-349 (2012).
- [31] C. Cattoen and M. Visser, arXiv:gr-qc/0703122 (2007).
- [32] O. Luongo, Mod. Phys. Lett. A **26**, 20, 1459-1466 (2011).
- [33] L. Xu and Y. Wang, Phys. Lett. B **702**, 114 (2011).
- [34] S. Capozziello and V. Salzano, Adv. Astron. **2009**, 1 (2009); O. Luongo, G. Iannone, and C. Autieri, Europh. Lett. **90**, 39001 (2010); G. Iannone and O. Luongo, Europh. Lett. **94**, 49002 (2011).
- [35] A. G. Riess *et al.*, Astrophys.J. **699**, 539 (2009); R. Jimenez, L. Verde, T. Treu, and D. Stern, Astrophys. J. **593**, 622-629 (2003).
- [36] A. Lewis and S. Bridle, Phys. Rev. D **66**, 103511 (2002).
- [37] T. Faber and M. Visser, Mon. Not. Roy. Astron. Soc. **372**, 136 (2006)
- [38] L. Xu and Y. Wang, Phys. Lett. B **702**, 114-120 (2011).
- [39] R. Nair, S. Jhingan, and D. Jain, JCAP **1105**, 023 (2011); B. A. Bassett and M. Kunz, Phys. Rev. D **69**, 101305 (2004).
- [40] I. M. H. Etherington, Gen. Rel. Grav. **39**, 1055 (2007); R. Kristian and R. K. Sachs, Astrophys. J. **143**, 379 (1966).
- [41] J. E. Taylor *et al.*, Astrophys. J. **749**, 127 (2012).
- [42] R. Amanullah *et al.* (SCP Collaboration), Astrophys. J. **716**, 712 (2010).
- [43] R. Lazkoz, S. Nesseris, and L. Perivolaropoulos, JCAP **0807**, 01 (2008); A. Avgoustidis, L. Verde, and R. Jimenez, JCAP **0906**, 012 (2009).
- [44] R. F. L. Holanda, J.A.S. Lima, and M. B. Ribeiro, Astron. Astrophys. **528**, L14 (2011); F. De Bernardis, E. Giusarma, and A. Melchiorri, Int. J. Mod. Phys. D **15**, 759 (2006).
- [45] G. F. R. Ellis, Gen. Rel. Grav. **39**, 1047 (2007).
- [46] A.G. Riess *et al.*, Astrophys. J. **699**, 539 (2009).
- [47] D. Stern, R. Jimenez, L. Verde, M. Kamionkowski, and S. A. Stanford, JCAP **1002**, 008 (2010).
- [48] J.-Q. Xia, V. Vitagliano, S. Liberati, and M. Viel, Phys. Rev. D **85**, 043520 (2012). S. Capozziello, R. Lazkoz, and V. Salzano, Phys. Rev. D **84**, 124061 (2011).
- [49] B. E. Schaefer, Astrophys. J. **660**, 16 (2007).
- [50] R. Durrer, arXiv:1103.5331 (2011).

## Appendix A: 5 Distances in terms of redshifts

### 1. Redshift $z$

We begin with the results for the cosmological distances for the conventional redshift  $z$ , starting with luminosity distance,

$$d_L = \frac{1}{H_0} \cdot \left[ z + z^2 \cdot \left( \frac{1}{2} - \frac{q_0}{2} \right) + z^3 \cdot \left( -\frac{1}{6} - \frac{j_0}{6} + \frac{q_0}{6} + \frac{q_0^2}{2} \right) + \right. \\ \left. + z^4 \cdot \left( \frac{1}{12} + \frac{5j_0}{24} - \frac{q_0}{12} + \frac{5j_0q_0}{12} - \frac{5q_0^2}{8} - \frac{5q_0^3}{8} + \frac{s_0}{24} \right) + \right. \\ \left. + z^5 \cdot \left( -\frac{1}{20} - \frac{9j_0}{40} + \frac{j_0^2}{12} - \frac{l_0}{120} + \frac{q_0}{20} - \frac{11j_0q_0}{12} + \frac{27q_0^2}{40} - \frac{7j_0q_0^2}{8} + \frac{11q_0^3}{8} + \frac{7q_0^4}{8} - \frac{11s_0}{120} - \frac{q_0s_0}{8} \right) + \right. \\ \left. + z^6 \cdot \left( \frac{1}{30} + \frac{7j_0}{30} - \frac{19j_0^2}{72} + \frac{19l_0}{720} + \frac{m_0}{720} - \frac{q_0}{30} + \frac{13j_0q_0}{9} - \frac{7j_0^2q_0}{18} + \frac{7l_0q_0}{240} - \frac{7q_0^2}{10} + \frac{133j_0q_0^2}{48} - \frac{13q_0^3}{6} + \right. \right. \\ \left. \left. + \frac{7j_0q_0^3}{4} - \frac{133q_0^4}{48} - \frac{21q_0^5}{16} + \frac{13s_0}{90} - \frac{7j_0s_0}{144} + \frac{19q_0s_0}{48} + \frac{7q_0^2s_0}{24} \right) \right],$$

the photon flux distance,

$$d_F = \frac{1}{H_0} \cdot \left[ z - z^2 \cdot \frac{q_0}{2} + z^3 \cdot \left( -\frac{1}{24} - \frac{j_0}{6} + \frac{5q_0}{12} + \frac{q_0^2}{2} \right) + \right. \\ \left. + z^4 \cdot \left( \frac{1}{24} + \frac{7j_0}{24} - \frac{17q_0}{48} + \frac{5j_0q_0}{12} - \frac{7q_0^2}{8} - \frac{5q_0^3}{8} + \frac{s_0}{24} \right) + \right. \\ \left. + z^5 \cdot \left( -\frac{71}{1920} - \frac{47j_0}{120} + \frac{j_0^2}{12} - \frac{l_0}{120} + \frac{149q_0}{480} - \frac{9j_0q_0}{8} + \frac{47q_0^2}{40} - \frac{7j_0q_0^2}{8} + \frac{27q_0^3}{16} + \frac{7q_0^4}{8} - \frac{9s_0}{80} - \frac{q_0s_0}{8} \right) + \right. \\ \left. + z^6 \cdot \left( \frac{31}{960} + \frac{457j_0}{960} - \frac{11j_0^2}{36} + \frac{11l_0}{360} + \frac{m_0}{720} - \frac{1069q_0}{3840} + \frac{593j_0q_0}{288} - \frac{7j_0^2q_0}{18} + \frac{7l_0q_0}{240} - \frac{457q_0^2}{320} + \frac{77j_0q_0^2}{24} + \right. \right. \\ \left. \left. - \frac{593q_0^3}{192} + \frac{7j_0q_0^3}{4} - \frac{77q_0^4}{24} - \frac{21q_0^5}{16} + \frac{593s_0}{2880} - \frac{7j_0s_0}{144} + \frac{11q_0s_0}{24} + \frac{7q_0^2s_0}{24} \right) \right],$$

the photon count distance,

$$d_P = \frac{1}{H_0} \cdot \left[ z + z^2 \cdot \left( -\frac{1}{2} - \frac{q_0}{2} \right) + z^3 \cdot \left( \frac{1}{3} - \frac{j_0}{6} + \frac{2q_0}{3} + \frac{q_0^2}{2} \right) + \right. \\ \left. + z^4 \cdot \left( -\frac{1}{4} + \frac{3j_0}{8} - \frac{3q_0}{4} + \frac{5j_0q_0}{12} - \frac{9q_0^2}{8} - \frac{5q_0^3}{8} + \frac{s_0}{24} \right) + \right. \\ \left. + z^5 \cdot \left( \frac{1}{5} - \frac{3j_0}{5} + \frac{j_0^2}{12} - \frac{l_0}{120} + \frac{4q_0}{5} - \frac{4j_0q_0}{3} + \frac{9q_0^2}{5} - \frac{7j_0q_0^2}{8} + 2q_0^3 + \frac{7q_0^4}{8} - \frac{2s_0}{15} - \frac{q_0s_0}{8} \right) + \right. \\ \left. + z^6 \cdot \left( -\frac{1}{6} + \frac{5j_0}{6} - \frac{25j_0^2}{72} + \frac{5l_0}{144} + \frac{m_0}{720} - \frac{5q_0}{6} + \frac{25j_0q_0}{9} - \frac{7j_0^2q_0}{18} + \frac{7l_0q_0}{240} - \frac{5q_0^2}{2} + \frac{175j_0q_0^2}{48} - \frac{25q_0^3}{6} + \right. \right. \\ \left. \left. + \frac{7j_0q_0^3}{4} - \frac{175q_0^4}{48} - \frac{21q_0^5}{16} + \frac{5s_0}{18} - \frac{7j_0s_0}{144} + \frac{25q_0s_0}{48} + \frac{7q_0^2s_0}{24} \right) \right],$$

the deceleration distance,

$$d_Q = \frac{1}{H_0} \cdot \left[ z + z^2 \cdot \left( -1 - \frac{q_0}{2} \right) + z^3 \cdot \left( \frac{23}{24} - \frac{j_0}{6} + \frac{11q_0}{12} + \frac{q_0^2}{2} \right) + \right. \\ \left. + z^4 \cdot \left( -\frac{11}{12} + \frac{11j_0}{24} - \frac{61q_0}{48} + \frac{5j_0q_0}{12} - \frac{11q_0^2}{8} - \frac{5q_0^3}{8} + \frac{s_0}{24} \right) + \right. \\ \left. + z^5 \cdot \left( \frac{563}{640} - \frac{17j_0}{20} + \frac{j_0^2}{12} - \frac{l_0}{120} + \frac{253q_0}{160} - \frac{37j_0q_0}{24} + \frac{51q_0^2}{20} - \frac{7j_0q_0^2}{8} + \frac{37q_0^3}{16} + \frac{7q_0^4}{8} - \frac{37s_0}{240} - \frac{q_0s_0}{8} \right) + \right. \\ \left. + z^6 \cdot \left( -\frac{1627}{1920} + \frac{1273j_0}{960} - \frac{7j_0^2}{18} + \frac{7l_0}{180} + \frac{m_0}{720} - \frac{7141q_0}{3840} + \frac{1037j_0q_0}{288} - \frac{7j_0^2q_0}{18} + \frac{7l_0q_0}{240} - \frac{1273q_0^2}{320} + \right. \right. \\ \left. \left. + \frac{49j_0q_0^2}{12} - \frac{1037q_0^3}{192} + \frac{7j_0q_0^3}{4} - \frac{49q_0^4}{12} - \frac{21q_0^5}{16} + \frac{1037s_0}{2880} - \frac{7j_0s_0}{144} + \frac{7q_0s_0}{12} + \frac{7q_0^2s_0}{24} \right) \right],$$

and the angular diameter distance,

$$\begin{aligned}
d_A = & \frac{1}{H_0} \cdot \left[ z + z^2 \cdot \left( -\frac{3}{2} - \frac{q_0}{2} \right) + z^3 \cdot \left( \frac{11}{6} - \frac{j_0}{6} + \frac{7q_0}{6} + \frac{q_0^2}{2} \right) + \right. \\
& + z^4 \cdot \left( -\frac{25}{12} + \frac{13j_0}{24} - \frac{23q_0}{12} + \frac{5j_0q_0}{12} - \frac{13q_0^2}{8} - \frac{5q_0^3}{8} + \frac{s_0}{24} \right) + \\
& + z^5 \cdot \left( \frac{137}{60} - \frac{137j_0}{120} + \frac{j_0^2}{12} - \frac{l_0}{120} + \frac{163q_0}{60} - \frac{7j_0q_0}{4} + \frac{137q_0^2}{40} - \frac{7j_0q_0^2}{8} + \frac{21q_0^3}{8} + \frac{7q_0^4}{8} - \frac{7s_0}{40} - \frac{q_0s_0}{8} \right) + \\
& + z^6 \cdot \left( -\frac{49}{20} + \frac{79j_0}{40} - \frac{31j_0^2}{72} + \frac{31l_0}{720} + \frac{m_0}{720} - \frac{71q_0}{20} + \frac{163j_0q_0}{36} - \frac{7j_0^2q_0}{18} + \frac{7l_0q_0}{240} - \frac{237q_0^2}{40} + \frac{217j_0q_0^2}{48} + \right. \\
& \left. - \frac{163q_0^3}{24} + \frac{7j_0q_0^3}{4} - \frac{217q_0^4}{48} - \frac{21q_0^5}{16} + \frac{163s_0}{360} - \frac{7j_0s_0}{144} + \frac{31q_0s_0}{48} + \frac{7q_0^2s_0}{24} \right) \Big].
\end{aligned}$$

## 2. Redshift $y_1$

Here we give the results for the distances in terms of  $y_1$ , first for the luminosity distance,

$$\begin{aligned}
d_L = & \frac{1}{H_0} \cdot \left[ y_1 + y_1^2 \cdot \left( \frac{3}{2} - \frac{q_0}{2} \right) + y_1^3 \cdot \left( \frac{11}{6} - \frac{j_0}{6} - \frac{5q_0}{6} + \frac{q_0^2}{2} \right) + \right. \\
& + y_1^4 \cdot \left( \frac{25}{12} - \frac{7j_0}{24} - \frac{13q_0}{12} + \frac{5j_0q_0}{12} + \frac{7q_0^2}{8} - \frac{5q_0^3}{8} + \frac{s_0}{24} \right) + \\
& + y_1^5 \cdot \left( \frac{137}{60} - \frac{47j_0}{120} + \frac{j_0^2}{12} - \frac{l_0}{120} - \frac{77q_0}{60} + \frac{3j_0q_0}{4} + \frac{47q_0^2}{40} - \frac{7j_0q_0^2}{8} - \frac{9q_0^3}{8} + \frac{7q_0^4}{8} + \frac{3s_0}{40} - \frac{q_0s_0}{8} \right) + \\
& + y_1^6 \cdot \left( \frac{49}{20} - \frac{19j_0}{40} + \frac{11j_0^2}{72} - \frac{11l_0}{720} + \frac{m_0}{720} - \frac{29q_0}{20} + \frac{37j_0q_0}{36} - \frac{7j_0^2q_0}{18} + \frac{7l_0q_0}{240} + \frac{57q_0^2}{40} - \frac{77j_0q_0^2}{48} - \frac{37q_0^3}{24} + \right. \\
& \left. + \frac{7j_0q_0^3}{4} + \frac{77q_0^4}{48} - \frac{21q_0^5}{16} + \frac{37s_0}{360} - \frac{7j_0s_0}{144} - \frac{11q_0s_0}{48} + \frac{7q_0^2s_0}{24} \right) \Big],
\end{aligned}$$

the photon flux distance,

$$\begin{aligned}
d_F = & \frac{1}{H_0} \cdot \left[ y_1 + y_1^2 \cdot \left( 1 - \frac{q_0}{2} \right) + y_1^3 \cdot \left( \frac{23}{24} - \frac{j_0}{6} - \frac{7q_0}{12} + \frac{q_0^2}{2} \right) + \right. \\
& + y_1^4 \cdot \left( \frac{11}{12} - \frac{5j_0}{24} - \frac{29q_0}{48} + \frac{5j_0q_0}{12} + \frac{5q_0^2}{8} - \frac{5q_0^3}{8} + \frac{s_0}{24} \right) + \\
& + y_1^5 \cdot \left( \frac{563}{640} - \frac{9j_0}{40} + \frac{j_0^2}{12} - \frac{l_0}{120} - \frac{97q_0}{160} + \frac{13j_0q_0}{24} + \frac{27q_0^2}{40} - \frac{7j_0q_0^2}{8} - \frac{13q_0^3}{16} + \frac{7q_0^4}{8} + \frac{13s_0}{240} - \frac{q_0s_0}{8} \right) + \\
& + y_1^6 \cdot \left( \frac{1627}{1920} - \frac{223j_0}{960} + \frac{j_0^2}{9} - \frac{l_0}{90} + \frac{m_0}{720} - \frac{2309q_0}{3840} + \frac{173j_0q_0}{288} - \frac{7j_0^2q_0}{18} + \frac{7l_0q_0}{240} + \frac{223q_0^2}{320} - \frac{7j_0q_0^2}{6} - \frac{173q_0^3}{192} + \right. \\
& \left. + \frac{7j_0q_0^3}{4} + \frac{7q_0^4}{6} - \frac{21q_0^5}{16} + \frac{173s_0}{2880} - \frac{7j_0s_0}{144} - \frac{q_0s_0}{6} + \frac{7q_0^2s_0}{24} \right) \Big],
\end{aligned}$$

the photon count distance,

$$\begin{aligned}
d_P = & \frac{1}{H_0} \cdot \left[ y_1 + y_1^2 \cdot \left( \frac{1}{2} - \frac{q_0}{2} \right) + y_1^3 \cdot \left( \frac{1}{3} - \frac{j_0}{6} - \frac{q_0}{3} + \frac{q_0^2}{2} \right) + \right. \\
& + y_1^4 \cdot \left( \frac{1}{4} - \frac{j_0}{8} - \frac{q_0}{4} + \frac{5j_0q_0}{12} + \frac{3q_0^2}{8} - \frac{5q_0^3}{8} + \frac{s_0}{24} \right) + \\
& + y_1^5 \cdot \left( \frac{1}{5} - \frac{j_0}{10} + \frac{j_0^2}{12} - \frac{l_0}{120} - \frac{q_0}{5} + \frac{j_0q_0}{3} + \frac{3q_0^2}{10} - \frac{7j_0q_0^2}{8} - \frac{q_0^3}{2} + \frac{7q_0^4}{8} + \frac{s_0}{30} - \frac{q_0s_0}{8} \right) + \\
& + y_1^6 \cdot \left( \frac{1}{6} - \frac{j_0}{12} + \frac{5j_0^2}{72} - \frac{l_0}{144} + \frac{m_0}{720} - \frac{q_0}{6} + \frac{5j_0q_0}{18} - \frac{7j_0^2q_0}{18} + \frac{7l_0q_0}{240} + \frac{q_0^2}{4} - \frac{35j_0q_0^2}{48} - \frac{5q_0^3}{12} + \frac{7j_0q_0^3}{4} + \right. \\
& \left. + \frac{35q_0^4}{48} - \frac{21q_0^5}{16} + \frac{s_0}{36} - \frac{7j_0s_0}{144} - \frac{5q_0s_0}{48} + \frac{7q_0^2s_0}{24} \right) \Big],
\end{aligned}$$

the deceleration distance,

$$\begin{aligned}
d_Q = & \frac{1}{H_0} \cdot \left[ y_1 - y_1^2 \cdot \frac{q_0}{2} + y_1^3 \cdot \left( -\frac{1}{24} - \frac{j_0}{6} - \frac{q_0}{12} + \frac{q_0^2}{2} \right) + \right. \\
& + y_1^4 \cdot \left( -\frac{1}{24} - \frac{j_0}{24} - \frac{q_0}{48} + \frac{5j_0q_0}{12} + \frac{q_0^2}{8} - \frac{5q_0^3}{8} + \frac{s_0}{24} \right) + \\
& + y_1^5 \cdot \left( -\frac{71}{1920} - \frac{j_0}{60} + \frac{j_0^2}{12} - \frac{l_0}{120} - \frac{q_0}{480} + \frac{j_0q_0}{8} + \frac{q_0^2}{20} - \frac{7j_0q_0^2}{8} - \frac{3q_0^3}{16} + \frac{7q_0^4}{8} + \frac{s_0}{80} - \frac{q_0s_0}{8} \right) + \\
& + y_1^6 \cdot \left( -\frac{31}{960} - \frac{7j_0}{960} + \frac{j_0^2}{36} - \frac{l_0}{360} + \frac{m_0}{720} + \frac{19q_0}{3840} + \frac{17j_0q_0}{288} - \frac{7j_0^2q_0}{18} + \frac{7l_0q_0}{240} + \frac{7q_0^2}{320} - \frac{7j_0q_0^2}{24} - \frac{17q_0^3}{192} + \right. \\
& \left. + \frac{7j_0q_0^3}{4} + \frac{7q_0^4}{24} - \frac{21q_0^5}{16} + \frac{17s_0}{2880} - \frac{7j_0s_0}{144} - \frac{q_0s_0}{24} + \frac{7q_0^2s_0}{24} \right) \Big],
\end{aligned}$$

and the angular diameter distance,

$$\begin{aligned}
d_A = & \frac{1}{H_0} \cdot \left[ y_1 + y_1^2 \cdot \left( -\frac{1}{2} - \frac{q_0}{2} \right) + y_1^3 \cdot \left( -\frac{1}{6} - \frac{j_0}{6} + \frac{q_0}{6} + \frac{q_0^2}{2} \right) + \right. \\
& + y_1^4 \cdot \left( -\frac{1}{12} + \frac{j_0}{24} + \frac{q_0}{12} + \frac{5j_0q_0}{12} - \frac{q_0^2}{8} - \frac{5q_0^3}{8} + \frac{s_0}{24} \right) + \\
& + y_1^5 \cdot \left( -\frac{1}{20} + \frac{j_0}{40} + \frac{j_0^2}{12} - \frac{l_0}{120} + \frac{q_0}{20} - \frac{j_0q_0}{12} - \frac{3q_0^2}{40} - \frac{7j_0q_0^2}{8} + \frac{q_0^3}{8} + \frac{7q_0^4}{8} - \frac{s_0}{120} - \frac{q_0s_0}{8} \right) + \\
& + y_1^6 \cdot \left( -\frac{1}{30} + \frac{j_0}{60} - \frac{j_0^2}{72} + \frac{l_0}{720} + \frac{m_0}{720} + \frac{q_0}{30} - \frac{j_0q_0}{18} - \frac{7j_0^2q_0}{18} + \frac{7l_0q_0}{240} - \frac{q_0^2}{20} + \frac{7j_0q_0^2}{48} + \frac{q_0^3}{12} + \frac{7j_0q_0^3}{4} + \right. \\
& \left. - \frac{7q_0^4}{48} - \frac{21q_0^5}{16} - \frac{s_0}{180} - \frac{7j_0s_0}{144} + \frac{q_0s_0}{48} + \frac{7q_0^2s_0}{24} \right) \Big].
\end{aligned}$$

### 3. Redshift $y_2$

The cosmological distances are given in terms of  $y_2$  - luminosity distance,

$$\begin{aligned}
d_L = & \frac{1}{H_0} \cdot \left[ y_2 + y_2^2 \cdot \left( \frac{3}{2} - \frac{q_0}{2} \right) + y_2^3 \cdot \left( \frac{13}{6} - \frac{j_0}{6} - \frac{5q_0}{6} + \frac{q_0^2}{2} \right) + \right. \\
& + y_2^4 \cdot \left( \frac{37}{12} - \frac{7j_0}{24} - \frac{17q_0}{12} + \frac{5j_0q_0}{12} - \frac{7q_0^2}{8} - \frac{5q_0^3}{8} + \frac{s}{24} \right) + \\
& + y_2^5 \cdot \left( \frac{17}{4} - \frac{67j_0}{120} + \frac{j_0^2}{12} - \frac{l_0}{120} - \frac{127q_0}{60} + \frac{3j_0q_0}{4} + \frac{67q_0^2}{40} - \frac{7j_0q_0^2}{8} - \frac{9q_0^3}{8} + \frac{7q_0^4}{8} + \frac{3s_0}{40} - \frac{q_0s_0}{8} \right) + \\
& + y_2^6 \cdot \left( \frac{1043}{180} - \frac{311j_0}{360} + \frac{11j_0^2}{72} - \frac{11l_0}{720} + \frac{m_0}{720} - \frac{37q_0}{12} + \frac{37j_0q_0}{9} - \frac{7j_0^2q_0}{36} - \frac{7l_0q_0}{240} - \frac{89q_0^2}{120} + \frac{21j_0q_0^2}{16} + \right. \\
& \left. + \frac{19q_0^3}{8} + \frac{7j_0q_0^3}{4} + \frac{77q_0^4}{48} - \frac{21q_0^5}{16} + \frac{19s_0}{120} - \frac{7j_0s_0}{144} - \frac{11q_0s_0}{48} + \frac{7q_0^2s_0}{24} \right) \Big],
\end{aligned}$$

the photon flux distance,

$$\begin{aligned}
d_F = & \frac{1}{H_0} \cdot \left[ y_2 + y_2^2 \cdot \left( 1 - \frac{q_0}{2} \right) + y_2^3 \cdot \left( \frac{31}{24} - \frac{j_0}{6} - \frac{7q_0}{12} + \frac{q_0^2}{2} \right) + \right. \\
& + y_2^4 \cdot \left( \frac{19}{12} - \frac{5j_0}{24} - \frac{15q_0}{16} + \frac{5j_0q_0}{12} + \frac{5q_0^2}{8} - \frac{5q_0^3}{8} + \frac{s_0}{24} \right) + \\
& + y_2^5 \cdot \left( \frac{757}{384} - \frac{47j_0}{120} + \frac{j_0^2}{12} - \frac{l_0}{120} - \frac{571q_0}{480} + \frac{13j_0q_0}{24} + \frac{47q_0^2}{40} - \frac{7j_0q_0^2}{8} - \frac{13q_0^3}{16} + \frac{7q_0^4}{8} + \frac{13s_0}{240} - \frac{q_0s_0}{8} \right) + \\
& + y_2^6 \cdot \left( \frac{4699}{1920} - \frac{1469j_0}{2880} + \frac{j_0^2}{9} - \frac{l_0}{90} + \frac{m_0}{720} - \frac{18383q_0}{11520} + \frac{37j_0q_0}{32} - \frac{7j_0^2q_0}{18} + \frac{7l_0q_0}{240} + \frac{1469q_0^2}{960} - \frac{7j_0q_0^2}{6} + \right. \\
& \left. - \frac{111q_0^3}{64} + \frac{7j_0q_0^3}{4} + \frac{7q_0^4}{6} - \frac{21q_0^5}{16} + \frac{37s_0}{320} - \frac{7j_0s_0}{144} - \frac{q_0s_0}{6} + \frac{7q_0^2s_0}{24} \right) \Big],
\end{aligned}$$



the photon count distance,

$$\begin{aligned}
d_P = & \frac{1}{H_0} \cdot \left[ y_2 + y_2^2 \cdot \left( \frac{1}{2} - \frac{q_0}{2} \right) + y_2^3 \cdot \left( \frac{2}{3} - \frac{j_0}{6} - \frac{q_0}{3} + \frac{q_0^2}{2} \right) + \right. \\
& + y_2^4 \cdot \left( \frac{7}{12} - \frac{j_0}{8} - \frac{7q_0}{12} + \frac{5j_0q_0}{12} + \frac{3q_0^2}{8} - \frac{5q_0^3}{8} + \frac{s_0}{24} \right) + \\
& + y_2^5 \cdot \left( \frac{2}{3} - \frac{4j_0}{15} + \frac{j_0^2}{12} - \frac{l_0}{120} - \frac{8q_0}{15} + \frac{j_0q_0}{3} + \frac{4q_0^2}{5} - \frac{7j_0q_0^2}{8} - \frac{q_0^3}{2} + \frac{7q_0^4}{8} + \frac{s_0}{30} - \frac{q_0s_0}{8} \right) + \\
& + y_2^6 \cdot \left( \frac{31}{45} - \frac{j_0}{4} + \frac{5j_0^2}{72} - \frac{l_0}{144} + \frac{m_0}{720} - \frac{31q_0}{45} + \frac{5j_0q_0}{6} - \frac{7j_0^2q_0}{18} + \frac{7l_0q_0}{240} + \frac{3q_0^2}{4} - \frac{35j_0q_0^2}{48} - \frac{5q_0^3}{4} + \right. \\
& \left. + \frac{7j_0q_0^3}{4} + \frac{35q_0^4}{48} - \frac{21q_0^5}{16} + \frac{s_0}{12} - \frac{7j_0s_0}{144} - \frac{5q_0s_0}{48} + \frac{7q_0^2s_0}{24} \right) \Big],
\end{aligned}$$

the deceleration distance,

$$\begin{aligned}
d_Q = & \frac{1}{H_0} \cdot \left[ y_2 - y_2^2 \cdot \frac{q_0}{2} + y_2^3 \cdot \left( \frac{7}{24} - \frac{j_0}{6} - \frac{q_0}{12} + \frac{q_0^2}{2} \right) + \right. \\
& + y_2^4 \cdot \left( -\frac{1}{24} - \frac{j_0}{24} - \frac{17q_0}{48} + \frac{5j_0q_0}{12} + \frac{q_0^2}{8} - \frac{5q_0^3}{8} + \frac{s_0}{24} \right) + \\
& + y_2^5 \cdot \left( \frac{7}{128} - \frac{11j_0}{60} + \frac{j_0^2}{12} - \frac{l_0}{120} - \frac{41q_0}{480} + \frac{j_0q_0}{8} + \frac{11q_0^2}{20} - \frac{7j_0q_0^2}{8} - \frac{3q_0^3}{16} + \frac{7q_0^4}{8} + \frac{s_0}{80} - \frac{q_0s_0}{8} \right) + \\
& + y_2^6 \cdot \left( -\frac{253}{2880} - \frac{181j_0}{2880} + \frac{j_0^2}{36} - \frac{l_0}{360} + \frac{m_0}{720} - \frac{271q_0}{1280} + \frac{59j_0q_0}{96} - \frac{7j_0^2q_0}{18} + \frac{7l_0q_0}{240} + \frac{181q_0^2}{960} - \frac{7j_0q_0^2}{24} - \right. \\
& \left. - \frac{59q_0^3}{64} + \frac{7j_0q_0^3}{4} + \frac{7q_0^4}{24} - \frac{21q_0^5}{16} + \frac{59s_0}{960} - \frac{7j_0s_0}{144} - \frac{q_0s_0}{24} + \frac{7q_0^2s_0}{24} \right) \Big],
\end{aligned}$$

and the angular diameter distance,

$$\begin{aligned}
d_A = & \frac{1}{H_0} \cdot \left[ y_2 + y_2^2 \cdot \left( -\frac{1}{2} - \frac{q_0}{2} \right) + y_2^3 \cdot \left( \frac{1}{6} - \frac{j_0}{6} + \frac{q_0}{6} + \frac{q_0^2}{2} \right) + \right. \\
& + y_2^4 \cdot \left( -\frac{5}{12} + \frac{j_0}{24} - \frac{q_0}{4} + \frac{5j_0q_0}{12} - \frac{q_0^2}{8} - \frac{5q_0^3}{8} + \frac{s_0}{24} \right) + \\
& + y_2^5 \cdot \left( -\frac{1}{12} - \frac{17j_0}{120} + \frac{j_0^2}{12} - \frac{l_0}{120} + \frac{13q_0}{60} - \frac{j_0q_0}{12} + \frac{17q_0^2}{40} - \frac{7j_0q_0^2}{8} + \frac{q_0^3}{8} + \frac{7q_0^4}{8} - \frac{s_0}{120} - \frac{q_0s_0}{8} \right) + \\
& + y_2^6 \cdot \left( -\frac{1}{3} + \frac{13j_0}{180} - \frac{j_0^2}{72} + \frac{l_0}{720} + \frac{m_0}{720} - \frac{2q_0}{45} + \frac{j_0q_0}{2} - \frac{7j_0^2q_0}{18} + \frac{7l_0q_0}{240} - \frac{13q_0^2}{60} + \frac{7j_0q_0^2}{48} - \frac{3q_0^3}{4} + \right. \\
& \left. + \frac{7j_0q_0^3}{4} - \frac{7q_0^4}{48} - \frac{21q_0^5}{16} + \frac{s_0}{20} - \frac{7j_0s_0}{144} + \frac{q_0s_0}{48} + \frac{7q_0^2s_0}{24} \right) \Big].
\end{aligned}$$

#### 4. Redshift $y_3$

These are the results for the cosmological distances in terms of the third redshift,  $y_3$ , beginning with the luminosity distance,

$$\begin{aligned}
d_L = & \frac{1}{H_0} \cdot \left[ y_3 + y_3^2 \cdot \left( \frac{1}{2} - \frac{q_0}{2} \right) + y_3^3 \cdot \left( \frac{5}{6} - \frac{j_0}{6} + \frac{q_0}{6} + \frac{q_0^2}{2} \right) + \right. \\
& + y_3^4 \cdot \left( \frac{13}{12} + \frac{5j_0}{24} - \frac{13q_0}{12} + \frac{5j_0q_0}{12} - \frac{5q_0^2}{8} - \frac{5q_0^3}{8} + \frac{s_0}{24} \right) + \\
& + y_3^5 \cdot \left( \frac{29}{20} - \frac{29j_0}{40} + \frac{j_0^2}{12} - \frac{l_0}{120} + \frac{11q_0}{20} - \frac{11j_0q_0}{12} - \frac{87q_0^2}{40} - \frac{7j_0q_0^2}{8} + \frac{11q_0^3}{8} + \frac{7q_0^4}{8} - \frac{11s_0}{120} - \frac{q_0s_0}{8} \right) + \\
& + y_3^6 \cdot \left( \frac{43}{15} + \frac{16j_0}{15} - \frac{19j_0^2}{72} + \frac{19l_0}{720} + \frac{m_0}{720} - \frac{43q_0}{15} + \frac{28j_0q_0}{9} - \frac{7j_0^2q_0}{18} + \frac{7l_0q_0}{240} - \frac{16q_0^2}{5} + \frac{133j_0q_0^2}{48} - \frac{14q_0^3}{3} + \right. \\
& \left. + \frac{7j_0q_0^3}{4} - \frac{133q_0^4}{48} - \frac{21q_0^5}{16} + \frac{14s_0}{45} - \frac{7j_0s_0}{144} + \frac{19q_0s_0}{48} + \frac{7q_0^2s_0}{24} \right) \Big],
\end{aligned}$$

the photon flux distance,

$$\begin{aligned}
d_F = & \frac{1}{H_0} \cdot \left[ y_3 - y_3^2 \cdot \frac{q_0}{2} + y_3^3 \cdot \left( \frac{23}{24} - \frac{j_0}{6} + \frac{5q_0}{12} + \frac{q_0^2}{2} \right) + \right. \\
& + y_3^4 \cdot \left( \frac{1}{24} + \frac{7j_0}{24} - \frac{65q_0}{48} + \frac{5j_0q_0}{12} - \frac{7q_0^2}{8} - \frac{5q_0^3}{8} + \frac{s_0}{24} \right) + \\
& + y_3^5 \cdot \left( \frac{3529}{1920} - \frac{107j_0}{120} + \frac{j_0^2}{12} - \frac{l_0}{120} + \frac{749q_0}{480} - \frac{9j_0q_0}{8} + \frac{107q_0^2}{40} - \frac{7j_0q_0^2}{8} + \frac{27q_0^3}{16} + \frac{7q_0^4}{8} - \frac{9s_0}{80} - \frac{q_0s_0}{8} \right) + \\
& + y_3^6 \cdot \left( \frac{191}{960} + \frac{1577j_0}{960} - \frac{11j_0^2}{36} + \frac{11l_0}{360} + \frac{m_0}{720} - \frac{16109q_0}{3840} + \frac{1073j_0q_0}{288} - \frac{7j_0^2q_0}{18} + \frac{7l_0q_0}{240} - \frac{1577q_0^2}{320} + \right. \\
& \left. + \frac{77j_0q_0^2}{24} - \frac{1073q_0^3}{192} + \frac{7j_0q_0^3}{4} - \frac{77q_0^4}{24} - \frac{21q_0^5}{16} + \frac{1073s_0}{2880} - \frac{7j_0s_0}{144} + \frac{11q_0s_0}{24} + \frac{7q_0^2s_0}{24} \right) \Big],
\end{aligned}$$

the photon count distance,

$$\begin{aligned}
d_P = & \frac{1}{H_0} \cdot \left[ y_3 + y_3^2 \cdot \left( -\frac{1}{2} - \frac{q_0}{2} \right) + y_3^3 \cdot \left( \frac{4}{3} - \frac{j_0}{6} + \frac{2q_0}{3} + \frac{q_0^2}{2} \right) + \right. \\
& + y_3^4 \cdot \left( -\frac{5}{4} + \frac{3j_0}{8} - \frac{7q_0}{4} + \frac{5j_0q_0}{12} - \frac{9q_0^2}{8} - \frac{5q_0^3}{8} + \frac{s_0}{24} \right) + \\
& + y_3^5 \cdot \left( \frac{16}{5} - \frac{11j_0}{10} + \frac{j_0^2}{12} - \frac{l_0}{120} + \frac{14q_0}{5} - \frac{4j_0q_0}{3} + \frac{33q_0^2}{10} - \frac{7j_0q_0^2}{8} + 2q_0^3 + \frac{7q_0^4}{8} - \frac{2s_0}{15} - \frac{q_0s_0}{8} \right) + \\
& + y_3^6 \cdot \left( -\frac{11}{3} + \frac{7j_0}{3} - \frac{25j_0^2}{72} + \frac{5l_0}{144} + \frac{m_0}{720} - \frac{19q_0}{3} + \frac{40j_0q_0}{9} - \frac{7j_0^2q_0}{18} + \frac{7l_0q_0}{240} - 7q_0^2 + \right. \\
& \left. + \frac{175j_0q_0^2}{48} - \frac{20q_0^3}{3} + \frac{7j_0q_0^3}{4} - \frac{175q_0^4}{48} - \frac{21q_0^5}{16} + \frac{4s_0}{9} - \frac{7j_0s_0}{144} + \frac{25q_0s_0}{48} + \frac{7q_0^2s_0}{24} \right) \Big],
\end{aligned}$$

the deceleration distance,

$$\begin{aligned}
d_Q = & \frac{1}{H_0} \cdot \left[ y_3 + y_3^2 \cdot \left( -1 - \frac{q_0}{2} \right) + y_3^3 \cdot \left( \frac{47}{24} - \frac{j_0}{6} + \frac{11q_0}{12} + \frac{q_0^2}{2} \right) + \right. \\
& + y_3^4 \cdot \left( -\frac{35}{12} + \frac{11j_0}{24} - \frac{109q_0}{48} + \frac{5j_0q_0}{12} - \frac{11q_0^2}{8} - \frac{5q_0^3}{8} + \frac{s_0}{24} \right) + \\
& + y_3^5 \cdot \left( \frac{3683}{640} - \frac{27j_0}{20} + \frac{j_0^2}{12} - \frac{l_0}{120} + \frac{693q_0}{160} - \frac{37j_0q_0}{24} + \frac{81q_0^2}{20} - \frac{7j_0q_0^2}{8} + \frac{37q_0^3}{16} + \frac{7q_0^4}{8} - \frac{37s_0}{240} - \frac{q_0s_0}{8} \right) + \\
& + y_3^6 \cdot \left( -\frac{6089}{640} + \frac{1011j_0}{320} - \frac{7j_0^2}{18} + \frac{7l_0}{18} + \frac{m_0}{720} - \frac{12087q_0}{1280} + \frac{1517j_0q_0}{288} - \frac{7j_0^2q_0}{18} + \frac{7l_0q_0}{240} - \frac{3033q_0^2}{320} + \right. \\
& \left. + \frac{49j_0q_0^2}{12} - \frac{1517q_0^3}{192} + \frac{7j_0q_0^3}{4} - \frac{49q_0^4}{12} - \frac{21q_0^5}{16} + \frac{1517s_0}{2880} - \frac{7j_0s_0}{144} + \frac{7q_0s_0}{12} + \frac{7q_0^2s_0}{24} \right) \Big],
\end{aligned}$$

and the angular diameter distance,

$$\begin{aligned}
d_A = & \frac{1}{H_0} \cdot \left[ y_3 + y_3^2 \cdot \left( -\frac{3}{2} - \frac{q_0}{2} \right) + y_3^3 \cdot \left( \frac{17}{6} - \frac{j_0}{6} + \frac{7q_0}{6} + \frac{q_0^2}{2} \right) + \right. \\
& + y_3^4 \cdot \left( -\frac{61}{12} + \frac{13j_0}{24} - \frac{35q_0}{12} + \frac{5j_0q_0}{12} - \frac{13q_0^2}{8} - \frac{5q_0^3}{8} + \frac{s_0}{24} \right) + \\
& + y_3^5 \cdot \left( \frac{587}{60} - \frac{197j_0}{120} + \frac{j_0^2}{12} - \frac{l_0}{120} + \frac{373q_0}{60} - \frac{7j_0q_0}{4} + \frac{197q_0^2}{40} - \frac{7j_0q_0^2}{8} + \frac{21q_0^3}{8} + \frac{7q_0^4}{8} - \frac{7s_0}{40} - \frac{q_0s_0}{8} \right) + \\
& + y_3^6 \cdot \left( -\frac{1097}{60} + \frac{497j_0}{120} - \frac{31j_0^2}{72} + \frac{31l_0}{720} + \frac{m_0}{720} - \frac{823q_0}{60} + \frac{223j_0q_0}{36} - \frac{7j_0^2q_0}{18} + \frac{7l_0q_0}{240} - \frac{497q_0^2}{40} + \right. \\
& \left. + \frac{217j_0q_0^2}{48} - \frac{223q_0^3}{24} + \frac{7j_0q_0^3}{4} - \frac{217q_0^4}{48} - \frac{21q_0^5}{16} + \frac{223s_0}{360} - \frac{7j_0s_0}{144} + \frac{31q_0s_0}{48} + \frac{7q_0^2s_0}{24} \right) \Big].
\end{aligned}$$

### 5. Redshift $y_4$

Finally, for the last redshift  $y_4$  the cosmological distances are given, starting with the luminosity distance,

$$\begin{aligned}
 d_L = & \frac{1}{H_0} \cdot \left[ y_4 + y_4^2 \cdot \left( \frac{1}{2} - \frac{q_0}{2} \right) + y_4^3 \cdot \left( \frac{1}{6} - \frac{j_0}{6} + \frac{q_0}{6} + \frac{q_0^2}{2} \right) + \right. \\
 & + y_4^4 \cdot \left( \frac{5}{12} + \frac{5j_0}{24} - \frac{5q_0}{12} + \frac{5j_0q_0}{12} - \frac{5q_0^2}{8} - \frac{5q_0^3}{8} + \frac{s_0}{24} \right) + \\
 & + y_4^5 \cdot \left( -\frac{1}{12} - \frac{47j_0}{120} + \frac{j_0^2}{12} - \frac{l_0}{120} + \frac{13q_0}{60} - \frac{11j_0q_0}{12} + \frac{47q_0^2}{40} - \frac{7j_0q_0^2}{8} + \frac{11q_0^3}{8} + \frac{7q_0^4}{8} - \frac{11s_0}{120} - \frac{q_0s_0}{8} \right) + \\
 & + y_4^6 \cdot \left( \frac{1}{3} + \frac{23j_0}{45} - \frac{19j_0^2}{72} + \frac{19l_0}{720} + \frac{m_0}{720} - \frac{q_0}{3} + 2j_0q_0 - \frac{7j_0^2q_0}{18} + \frac{7l_0q_0}{240} - \frac{23q_0^2}{15} + \frac{133j_0q_0^2}{48} - 3q_0^3 + \right. \\
 & \left. \left. + \frac{7j_0q_0^3}{4} - \frac{133q_0^4}{48} - \frac{21q_0^5}{16} + \frac{s_0}{5} - \frac{7j_0s_0}{144} + \frac{19q_0s_0}{48} + \frac{7q_0^2s_0}{24} \right) \right],
 \end{aligned}$$

the photon flux distance,

$$\begin{aligned}
 d_F = & \frac{1}{H_0} \cdot \left[ y_4 - y_4^2 \cdot \frac{q_0}{2} + y_4^3 \cdot \left( \frac{7}{24} - \frac{j_0}{6} + \frac{5q_0}{12} + \frac{q_0^2}{2} \right) + \right. \\
 & + y_4^4 \cdot \left( \frac{1}{24} + \frac{7j_0}{24} - \frac{11q_0}{16} + \frac{5j_0q_0}{12} - \frac{7q_0^2}{8} - \frac{5q_0^3}{8} + \frac{s_0}{24} \right) + \\
 & + y_4^5 \cdot \left( \frac{7}{128} - \frac{67j_0}{120} + \frac{j_0^2}{12} - \frac{l_0}{120} + \frac{349q_0}{480} - \frac{9j_0q_0}{8} + \frac{67q_0^2}{40} - \frac{7j_0q_0^2}{8} + \frac{27q_0^3}{16} + \frac{7q_0^4}{8} - \frac{9s_0}{80} - \frac{q_0s_0}{8} \right) + \\
 & + y_4^6 \cdot \left( \frac{253}{2880} + \frac{2491j_0}{2880} - \frac{11j_0^2}{36} + \frac{11l_0}{360} + \frac{m_0}{720} - \frac{10823q_0}{11520} + \frac{251j_0q_0}{96} - \frac{7j_0^2q_0}{18} + \frac{7l_0q_0}{240} - \frac{2491q_0^2}{960} + \right. \\
 & \left. \left. + \frac{77j_0q_0^2}{24} - \frac{251q_0^3}{64} + \frac{7j_0q_0^3}{4} - \frac{77q_0^4}{24} - \frac{21q_0^5}{16} + \frac{251s_0}{960} - \frac{7j_0s_0}{144} + \frac{11q_0s_0}{24} + \frac{7q_0^2s_0}{24} \right) \right],
 \end{aligned}$$

the photon count distance,

$$\begin{aligned}
 d_P = & \frac{1}{H_0} \cdot \left[ y_4 + y_4^2 \cdot \left( -\frac{1}{2} - \frac{q_0}{2} \right) + y_4^3 \cdot \left( \frac{2}{3} - \frac{j_0}{6} + \frac{2q_0}{3} + \frac{q_0^2}{2} \right) + \right. \\
 & + y_4^4 \cdot \left( -\frac{7}{12} + \frac{3j_0}{8} - \frac{13q_0}{12} + \frac{5j_0q_0}{12} - \frac{9q_0^2}{8} - \frac{5q_0^3}{8} + \frac{s_0}{24} \right) + \\
 & + y_4^5 \cdot \left( \frac{2}{3} - \frac{23j_0}{30} + \frac{j_0^2}{12} - \frac{l_0}{120} + \frac{22q_0}{15} - \frac{4j_0q_0}{3} + \frac{23q_0^2}{10} - \frac{7j_0q_0^2}{8} + 2q_0^3 + \frac{7q_0^4}{8} - \frac{2s_0}{15} - \frac{q_0s_0}{8} \right) + \\
 & + y_4^6 \cdot \left( -\frac{31}{45} + \frac{4j_0}{3} - \frac{25j_0^2}{72} + \frac{5l_0}{144} + \frac{m_0}{720} - \frac{91q_0}{45} + \frac{10j_0q_0}{3} - \frac{7j_0^2q_0}{18} + \frac{7l_0q_0}{240} - 4q_0^2 + \frac{175j_0q_0^2}{48} - 5q_0^3 + \right. \\
 & \left. \left. + \frac{7j_0q_0^3}{4} - \frac{175q_0^4}{48} - \frac{21q_0^5}{16} + \frac{s_0}{3} - \frac{7j_0s_0}{144} + \frac{25q_0s_0}{48} + \frac{7q_0^2s_0}{24} \right) \right],
 \end{aligned}$$

the deceleration distance,

$$\begin{aligned}
 d_Q = & \frac{1}{H_0} \cdot \left[ y_4 + y_4^2 \cdot \left( -1 - \frac{q_0}{2} \right) + y_4^3 \cdot \left( \frac{31}{24} - \frac{j_0}{6} + \frac{11q_0}{12} + \frac{q_0^2}{2} \right) + \right. \\
 & + y_4^4 \cdot \left( -\frac{19}{12} + \frac{11j_0}{24} - \frac{77q_0}{48} + \frac{5j_0q_0}{12} - \frac{11q_0^2}{8} - \frac{5q_0^3}{8} + \frac{s_0}{24} \right) + \\
 & + y_4^5 \cdot \left( \frac{757}{384} - \frac{61j_0}{60} + \frac{j_0^2}{12} - \frac{l_0}{120} + \frac{1199q_0}{480} - \frac{37j_0q_0}{24} + \frac{61q_0^2}{20} - \frac{7j_0q_0^2}{8} + \frac{37q_0^3}{16} + \frac{7q_0^4}{8} - \frac{37s_0}{240} - \frac{q_0s_0}{8} \right) + \\
 & + y_4^6 \cdot \left( -\frac{4699}{1920} + \frac{5579j_0}{2880} - \frac{7j_0^2}{18} + \frac{7l_0}{180} + \frac{m_0}{720} - \frac{4791q_0}{1280} + \frac{133j_0q_0}{32} - \frac{7j_0^2q_0}{18} + \frac{7l_0q_0}{240} - \frac{5579q_0^2}{960} + \right. \\
 & \left. \left. + \frac{49j_0q_0^2}{12} - \frac{399q_0^3}{64} + \frac{7j_0q_0^3}{4} - \frac{49q_0^4}{12} - \frac{21q_0^5}{16} + \frac{133s_0}{320} - \frac{7j_0s_0}{144} + \frac{7q_0s_0}{12} + \frac{7q_0^2s_0}{24} \right) \right],
 \end{aligned}$$

and the angular diameter distance,

$$\begin{aligned}
d_A = & \frac{1}{H_0} \cdot \left[ y_4 + y_4^2 \cdot \left( -\frac{3}{2} - \frac{q_0}{2} \right) + y_4^3 \cdot \left( \frac{13}{6} - \frac{j_0}{6} + \frac{7q_0}{6} + \frac{q_0^2}{2} \right) + \right. \\
& + y_4^4 \cdot \left( -\frac{37}{12} + \frac{13j_0}{24} - \frac{9q_0}{4} + \frac{5j_0q_0}{12} - \frac{13q_0^2}{8} - \frac{5q_0^3}{8} + \frac{s_0}{24} \right) + \\
& + y_4^5 \cdot \left( \frac{17}{4} - \frac{157j_0}{120} + \frac{j_0^2}{12} - \frac{l_0}{120} + \frac{233q_0}{60} - \frac{7j_0q_0}{4} + \frac{157q_0^2}{40} - \frac{7j_0q_0^2}{8} + \frac{21q_0^3}{8} + \frac{7q_0^4}{8} - \frac{7s_0}{40} - \frac{q_0s_0}{8} \right) + \\
& + y_4^6 \cdot \left( -\frac{1043}{180} + \frac{971j_0}{360} - \frac{31j_0^2}{72} + \frac{31l_0}{720} + \frac{m_0}{720} - \frac{1133q_0}{180} + \frac{61j_0q_0}{12} - \frac{7j_0^2q_0}{18} + \frac{7l_0q_0}{240} - \frac{971q_0^2}{120} + \right. \\
& \left. + \frac{217j_0q_0^2}{48} - \frac{61q_0^3}{8} + \frac{7j_0q_0^3}{4} - \frac{217q_0^4}{48} - \frac{21q_0^5}{16} + \frac{61s_0}{120} - \frac{7j_0s_0}{144} + \frac{31q_0s_0}{48} + \frac{7q_0^2s_0}{24} \right) \Big].
\end{aligned}$$

### Appendix B: The Hubble parameter as a function of redshifts

We start with the parametrization of the Hubble parameter in terms of the commonly used redshift  $z$ , given by

$$\begin{aligned}
H(z) = & H_0 \cdot \left[ 1 + z \cdot (1 + q_0) + \frac{z^2}{2} \cdot (j_0 - q_0^2) + \frac{z^3}{6} \cdot (-3q_0^2 - 3q_0^3 + j_0(3 + 4q_0) + s_0) + \right. \\
& + \frac{z^4}{24} \cdot (-4j_0^2 + l_0 - 12q_0^2 - 24q_0^3 - 15q_0^4 + j_0(12 + 32q_0 + 25q_0^2) + 8s_0 + 7q_0s_0) + \\
& + \frac{z^5}{120} \cdot (m_0 - 60q_0^2 - 180q_0^3 - 225q_0^4 - 105q_0^5 - 10j_0^2(6 + 7q_0) + l_0(15 + 11q_0) + \\
& \left. + 15j_0(4 + 16q_0 + 25q_0^2 + 14q_0^3 - s_0) + 60s_0 + 105q_0s_0 + 60q_0^2s_0) \right].
\end{aligned}$$

Further we calculated the expression  $H(y_1)$ , as

$$\begin{aligned}
H(y_1) = & H_0 \cdot \left[ 1 + y_1 \cdot (1 + q_0) + \frac{y_1^2}{2} \cdot (2 + j_0 + 2q_0 - q_0^2) + \frac{y_1^3}{6} \cdot (-6 - 6q_0 + 3q_0^2 - 3q_0^3 + j_0(-3 + 4q_0) + s_0) + \right. \\
& + \frac{y_1^4}{24} \cdot (24 - 4j_0^2 + l_0 + 24q_0 - 12q_0^2 + 12q_0^3 - 15q_0^4 + j_0(12 - 16q_0 + 25q_0^2) - 4s_0 + 7q_0s_0) + \\
& + \frac{y_1^5}{120} \cdot (-120 + m_0 + j_0^2(20 - 70q_0) - 120q_0 + 60q_0^2 - 60q_0^3 + 75q_0^4 - 105q_0^5 + l_0(-5 + 11q_0) + \\
& \left. + 20s_0 - 35q_0s_0 + 60q_0^2s_0 + 5j_0(16q_0 - 25q_0^2 + 42q_0^3 - 3(4 + s_0))) \right],
\end{aligned}$$

and in terms of the third redshift,  $H(y_4)$ ,

$$\begin{aligned}
H(y_4) = & H_0 \cdot \left[ 1 + y_4 \cdot (1 + q_0) + \frac{y_4^2}{2} \cdot (j_0 - q_0^2) + \frac{y_4^3}{6} \cdot (-2 + 3j_0 - 2q_0 + 4j_0q_0 - 3q_0^2 - 3q_0^3 + s_0) + \right. \\
& + \frac{y_4^4}{48} \cdot (8 + 32j_0 - 8j_0^2 + 2l_0 + 8q_0 + 16j_0q_0 - 40q_0^2 + 50j_0q_0^2 - 48q_0^3 - 30q_0^4 - 8(1 + q_0) + \\
& + 8j_0(1 + 6q_0) + 16s_0 + 14q_0s_0) + \\
& + \frac{y_4^5}{240} \cdot (-222 - 15j_0 - 40j_0^2 + 10l_0 + 2m_0 - 222q_0 + 400j_0q_0 - 140j_0^2q_0 + 22l_0q_0 + 15q_0^2 + \\
& + 250j_0q_0^2 - 300q_0^3 + 420j_0q_0^3 - 150q_0^4 - 210q_0^5 + 60(1 + j_0 + q_0 - q_0^2) + 100s_0 - 30j_0s_0 + \\
& + 70q_0s_0 + 120q_0^2s_0 - 5(-26 + 16j_0^2 - 4l_0 - 26q_0 + 39q_0^2 + 36q_0^3 + 60q_0^4 - j_0(39 + 48q_0 + 100q_0^2) + \\
& \left. - 12s_0 - 28q_0s_0)) \right].
\end{aligned}$$

### Appendix C: Pressure and derivatives as function of redshifts

In this section we give the expressions for the pressure in terms of the three redshifts, and also its derivatives with respect to these redshifts, evaluated at present cosmic time  $t_0$ , which is equivalent to  $z = y_1 = y_4 = 0$ .



The result for the pressure in terms of  $z$  reads

$$\begin{aligned}
P(z=0) &= \frac{1}{3}H_0^2(-1+2q_0), \\
\left.\frac{dP}{dz}\right|_{z=0} &= \frac{2}{3}H_0^2(-1+j_0), \\
\left.\frac{d^2P}{dz^2}\right|_{z=0} &= -\frac{2}{3}H_0^2(1+j_0+2q_0+j_0q_0+s_0), \\
\left.\frac{d^3P}{dz^3}\right|_{z=0} &= \frac{2}{3}H_0^2(-j_0^2+l_0+j_0q_0(4+3q_0)+(4+3q_0)s_0), \\
\left.\frac{d^4P}{dz^4}\right|_{z=0} &= \frac{2}{3}H_0^2(9j_0^2-9l_0-m_0-16j_0q_0+10j_0^2q_0-6l_0q_0-27j_0q_0^2-15j_0q_0^3-16s_0+5j_0s_0-27q_0s_0-15q_0^2s_0),
\end{aligned}$$

expressed in terms of  $y_1$  we have

$$\begin{aligned}
P(y_1=0) &= \frac{1}{3}H_0^2(-1+2q_0), \\
\left.\frac{dP}{dy_1}\right|_{y_1=0} &= \frac{2}{3}H_0^2(-1+j_0), \\
\left.\frac{d^2P}{dy_1^2}\right|_{y_1=0} &= -\frac{2}{3}H_0^2(3+j_0(-1+q_0)+2q_0+s_0), \\
\left.\frac{d^3P}{dy_1^3}\right|_{y_1=0} &= -\frac{2}{3}H_0^2(12+j_0^2-l_0+12q_0+j_0(2-3q_0)q_0+2s_0-3q_0s_0), \\
\left.\frac{d^4P}{dy_1^4}\right|_{y_1=0} &= -\frac{2}{3}H_0^2(60+m_0+j_0^2(3-10q_0)+72q_0+l_0(-3+6q_0)+j_0(12+4q_0-9q_0^2+15q_0^3-5s_0)+ \\
&\quad +4s_0-9q_0s_0+15q_0^2s_0),
\end{aligned}$$

and finally with respect to  $y_4$ , the results for the pressure and its derivatives are

$$\begin{aligned}
P(y_4=0) &= \frac{1}{3}H_0^2(-1+2q_0), \\
\left.\frac{dP}{dy_4}\right|_{y_4=0} &= \frac{2}{3}H_0^2(-1+j_0), \\
\left.\frac{d^2P}{dy_4^2}\right|_{y_4=0} &= -\frac{2}{3}H_0^2(1+j_0+2q_0+j_0q_0+s_0), \\
\left.\frac{d^3P}{dy_4^3}\right|_{y_4=0} &= -\frac{2}{3}H_0^2(2-2j_0+j_0^2-l_0-4j_0q_0-3j_0q_0^2-4s_0-3q_0s_0), \\
\left.\frac{d^4P}{dy_4^4}\right|_{y_4=0} &= \frac{1}{3}H_0^2(-24-8(-1+j_0)-11j_0+18j_0^2-18l_0-2m_0-32q_0-28j_0q_0+20j_0^2q_0-12l_0q_0-18j_0q_0^2+ \\
&\quad -30j_0q_0^3+j_0(3-20q_0-36q_0^2)-48s_0+10j_0s_0-54q_0s_0-30q_0^2s_0).
\end{aligned}$$

#### Appendix D: Luminosity distance as function of the EoS parametrization

These are the expressions for the luminosity distance  $d_L$  in terms not of the CS, but in terms of the pressure and its derivatives with respect to redshift. To make the equations more readable, we introduce the notions  $P_1 = \frac{dP}{dy_i}$ ,  $P_2 = \frac{d^2P}{dy_i^2}$  etc., where  $y_i = z, y_1, y_4$ .

For redshift  $z$  we have

$$\begin{aligned}
d_L(z) = & \frac{1}{H_0} \cdot \left[ z + \frac{z^2}{4} \cdot (1 - 3\omega) + z^3 \cdot \left( -\frac{1}{8} - \frac{P_1}{4H_0^2} + \omega + \frac{9\omega^2}{8} \right) + \right. \\
& + \frac{z^4}{64H_0^2} \cdot \left( -4P_2 + P_1 \cdot (34 + 54\omega) - 5H_0^2 (-1 + 17\omega + 45\omega^2 + 27\omega^3) \right) + \\
& + \frac{z^5}{640H_0^4} \cdot \left( 108P_1^2 + 5H_0^4 (-7 + 218\omega + 1008\omega^2 + 1350\omega^3 + 567\omega^4) + \right. \\
& - 4H_0^2 (-26P_2 + 2P_3 - 36P_2\omega + P_1 (136 + 531\omega + 405\omega^2)) \left. \right) + \\
& + \frac{z^6}{7680H_0^6} \cdot \left( -45H_0^4 (1 + \omega)^2 (-7 + 375\omega + 1827\omega^2 + 1701\omega^3) + 4H_0^2 \cdot 9P_1 (257 + 1817\omega + 3135\omega^2 + \right. \\
& \left. + 1575\omega^3) - 36P_1 (-20P_2 + P_1 (169 + 225\omega)) - 8H_0^2 [2P_4 - 5P_3 (7 + 9\omega) + 9P_2 (31 + 106\omega + 75\omega^2)] \right) \left. \right],
\end{aligned}$$

for redshift  $y_1$  the luminosity distance is given by

$$\begin{aligned}
d_L(y_1) = & \frac{1}{H_0} \cdot \left[ y_1 + \frac{y_1^2}{4} \cdot (5 - 3\omega) + \frac{y_1^3}{8} \cdot \left( 11 - \frac{2P_1}{H_0^2} - 4\omega + 9\omega^2 \right) + \right. \\
& - \frac{y_1^4}{64H_0^2} \cdot \left( 4P_2 + P_1 (6 - 54\omega) + H_0^2 (-93 + 37\omega + 9\omega^2 + 135\omega^3) \right) + \\
& + \frac{y_1^5}{640H_0^4} \cdot \left( 108P_1^2 + 5H_0^4 (193 - 78\omega + 72\omega^2 + 270\omega^3 + 567\omega^4) - 4H_0^2 (2(P_2 + P_3 - 18P_2\omega) + \right. \\
& \left. + P_1 (20 + 63\omega + 405\omega^2)) \right) + \\
& + \frac{y_1^6}{7680H_0^6} \cdot \left( -15H_0^4 (-793 + 323\omega - 210\omega^2 + 990\omega^3 + 4347\omega^4 + 5103\omega^5) + 36P_1 (-20P_2 + P_1 (29 + \right. \\
& \left. + 225\omega)) + 4H_0^2 (3P_1 (-85 + 243\omega + 2205\omega^2 + 4725\omega^3) - 2(P_3 + 2P_4 - 45P_3\omega + 3P_2 (7 + 48\omega + 225\omega^2))) \right) \left. \right],
\end{aligned}$$

and for the last redshift  $y_4$  the result reads

$$\begin{aligned}
d_L(y_4) = & \frac{1}{H_0} \cdot \left[ y_4 + \frac{y_4^2}{4} \cdot (1 - 3\omega) + y_4^3 \cdot \left( \frac{5}{24} - \frac{P_1}{4H_0^2} + \omega + \frac{9\omega^2}{8} \right) + \right. \\
& + \frac{y_4^4}{192H_0^2} \cdot \left( -H_0^2 (-47 + 351\omega + 675\omega^2 + 405\omega^3) + 6 (-2P_2 + P_1 (17 + 27\omega)) \right) + \\
& + \frac{y_4^5}{1920H_0^4} \cdot \left( 324P_1^2 + H_0^4 (-89 + 5190\omega + 17280\omega^2 + 20250\omega^3 + 8505\omega^4) + \right. \\
& - 12H_0^2 (-26P_2 + 2P_3 - 36P_2\omega + P_1 (172 + 531\omega + 405\omega^2)) \left. \right) + \\
& + \frac{y_4^6}{23040H_0^6} \cdot \left( H_0^4 (-5521 + 96063\omega + 454950\omega^2 + 838350\omega^3 + 705915\omega^4 + 229635\omega^5) + \right. \\
& - 12H_0^2 [P_1 (3533 + 18333\omega + 28215\omega^2 + 14175\omega^3) - 2 (2P_4 - 5P_3 (7 + 9\omega) + P_2 (343 + 954\omega + 675\omega^2))] + \\
& \left. + 108P_1 (-20P_2 + P_1 (169 + 225\omega)) \right) \left. \right].
\end{aligned}$$

### Appendix E: Derivatives of $G(z)$

Here we report the results for the derivatives of the function  $G(z)$ , which characterizes the equation of state of dark energy in a specific model, evaluated at present time, for the three redshifts under consideration.

The derivatives with respect to redshift  $z$  at  $z = 0$  read

$$\begin{aligned}
\left. \frac{dG}{dz} \right|_{z=0} &= 2 - 3\Omega_m + 2q_0, \\
\left. \frac{d^2G}{dz^2} \right|_{z=0} &= -2(-1 - j_0 + 3\Omega_m - 2q_0), \\
\left. \frac{d^3G}{dz^3} \right|_{z=0} &= -2(3\Omega_m + j_0q_0 + s_0), \\
\left. \frac{d^4G}{dz^4} \right|_{z=0} &= 2(-12j_0 + 3j_0^2 + 12j_0\Omega_m - 4j_0^2\Omega_m + l_0\Omega_m - 28j_0q_0 + 32j_0\Omega_mq_0 + 12q_0^2 - 22j_0q_0^2 + \\
&\quad - 12\Omega_mq_0^2 + 25j_0\Omega_mq_0^2 + 24q_0^3 - 24\Omega_mq_0^3 + 15q_0^4 - 15\Omega_mq_0^4 - 4s_0 + 8\Omega_ms_0 - 4q_0s_0 + \\
&\quad + 7\Omega_mq_0s_0 + (1 - \Omega_m)(-4j_0^2 + l_0 - 12q_0^2 - 24q_0^3 - 15q_0^4 + j_0(12 + 32q_0 + 25q_0^2) + 8s_0 + 7q_0s_0)), \\
\left. \frac{d^5G}{dz^5} \right|_{z=0} &= -2(10l_0 + m_0 + 6l_0q_0 - 10j_0^2(1 + q_0) + 5j_0(4q_0 + 6q_0^2 + 3q_0^3 - s_0) + 20s_0 + 30q_0s_0 + 15q_0^2s_0),
\end{aligned}$$

expressed in terms of  $y_1$  we have at  $y_1 = 0$

$$\begin{aligned}
\left. \frac{dG}{dy_1} \right|_{y_1=0} &= 2 - 3\Omega_m + 2q_0, \\
\left. \frac{d^2G}{dy_1^2} \right|_{y_1=0} &= -2(-2 - j_0 + 6\Omega_m - 2q_0 + q_0^2 - (1 + q_0)^2), \\
\left. \frac{d^3G}{dy_1^3} \right|_{y_1=0} &= -2(-6 + 30\Omega_m - 6q_0 + 3q_0^2 - 3q_0^3 + j_0(-3 + 4q_0) - 3(1 + q_0)(2 + j_0 + 2q_0 - q_0^2) + s_0),
\end{aligned}$$

and finally with respect to  $y_4$ , the results for the derivatives at present time  $y_4 = 0$  are

$$\begin{aligned}
\left. \frac{dG}{dy_4} \right|_{y_4=0} &= 2 - 3\Omega_m + 2q_0, \\
\left. \frac{d^2G}{dy_4^2} \right|_{y_4=0} &= 2(1 + j_0 - 3\Omega_m + 2q_0), \\
\left. \frac{d^3G}{dy_4^3} \right|_{y_4=0} &= -2(-2 + 6\Omega_m + (-2 + j_0)q_0 + s_0), \\
\left. \frac{d^4G}{dy_4^4} \right|_{y_4=0} &= 2(8 - j_0^2 + l_0 - 24\Omega_m + 16q_0 + j_0(8 + 4q_0 + 3q_0^2) + 4s_0 + 3q_0s_0), \\
\left. \frac{d^5G}{dy_4^5} \right|_{y_4=0} &= -2(-16 + m_0 + 84\Omega_m - 16q_0 - 10j_0^2(1 + q_0) + 2l_0(5 + 3q_0) + 5j_0(8q_0 + 6q_0^2 + 3q_0^3 - s_0) + \\
&\quad + 40s_0 + 30q_0s_0 + 15q_0^2s_0).
\end{aligned}$$


---